

**Carbon Dots Composites for Bioapplications: A Review**

Journal:	<i>Journal of Materials Chemistry B</i>
Manuscript ID	TB-REV-11-2021-002446.R1
Article Type:	Review Article
Date Submitted by the Author:	09-Dec-2021
Complete List of Authors:	Wu, Jiajia; Yunnan University, School of Materials and Energy Chen, Gonglin; Yunnan University, School of Materials and Energy Jia, Yinnong; Kunming Medical University Ji, Chunyu; Yunnan University, School of Materials and Energy Wang, Yuting; Kunming Medical University Zhou, Yiqun; University of Miami, Chemistry Leblanc, Roger; University of Miami, Department of Chemistry Peng, Zhili; Yunnan University, School of Materials and Energy

Carbon Dots Composites for Bioapplications: A Review

Jiajia Wu,^a Gonglin Chen,^a Yinnong Jia,^b Chunyu Ji,^a Yuting Wang,^b Yiqun Zhou,^c
Roger M. Leblanc,^c and Zhili Peng^{*a}

^aSchool of Materials and Energy, Yunnan University, Kunming 650091, People's Republic of China.

^bYunnan Provincial Key Laboratory of Pharmacology for Natural Products, School of Pharmaceutical Sciences, Kunming Medical University, Kunming 650500, People's Republic of China.

^cDepartment of Chemistry, University of Miami, 1301 Memorial Drive, Coral Gables, Florida 33146, United States.

***Corresponding authors:**

(Z. P.) Tel.: +86–871–65037399; E-mail: zhilip@ynu.edu.cn.

Keywords:

Carbon dots; composites; bioimaging; drug delivery; biosensing;

Abstract

Carbon dots (CDs) have received extensive attention in the last decade for their excellent optical, chemical and biological properties. In recent years, CDs composites have also received significant attention due to their ability to improve the intrinsic properties and expand the application scopes of CDs. In this article, the syntheses of four types of CDs composites (metal-CDs, nonmetallic inorganics-CDs, organics-CDs as well as multi-components-CDs composites) are systematically summarized first. Then the recent advancements on the bioapplications (bioimaging, drug delivery and biosensing) of these composites are also highlighted and discussed. Last, current challenges and future trends of CDs composites in the biomedical fields are discussed.

1. Introduction

Carbon dots (CDs) are a group of quasi-spherical nanoparticles with sizes smaller than 10 nm¹, which were first discovered accidentally in 2004 by researchers from the United States during the separation and purification of single-walled carbon nanotubes (SWCNTs) by gel electrophoresis². CDs did not receive enough attention until a groundbreaking report from Sun's group in 2006³. Structurally speaking, CDs are generally considered to possess carbonized cores (either crystalline or amorphous) with functionalized surfaces which could contain various functionalities such as carbonyls, carboxylic acids, hydroxyls, epoxides, amines and etc.⁴⁻⁶. The nature and properties of CDs surfaces are easily influenced by the precursors used and synthesis methods adopted during the synthesis of CDs^{7, 8}, thus rendering CDs with the advantage of facile surface modifications. Syntheses for CDs are simple and versatile, which could be classified into two approaches, namely "top-down" and "bottom-up"⁹. In "top-down" method, it generally involves the cleavage of large carbonaceous materials into small CDs *via* harsh treatments such as arc discharge, laser ablation^{10, 11}, electrochemical stripping¹² as well as acidic oxidation treatment^{13, 14}. In "bottom-up" approach, it involves the polymerization and carbonization of small carbon-containing molecules into CDs¹⁵, which could be realized through microwave¹⁶ or hydrothermal/solvothermal treatments¹⁷.

In the past decade, the field of CDs has advanced significantly, as evidenced by their wide applications in various fields such as chemistry, physics, engineering and optoelectronics¹⁸⁻²⁰. Among them, CDs are especially known for their cross applications in the biomedical fields considering their unique photoluminescence (PL) properties, excellent photostability, extraordinary biocompatibility, tunable surface functionalities, facile syntheses, as well as economic accessibility²¹⁻²⁵. As a result, CDs have been widely investigated for their potential applications for bioimaging, biosensing as well as drug and gene delivery²⁶⁻³¹ in the last decade (**Figure 1**). In light of the emerging studies on the biomedical applications of CDs, various excellent review articles have been published on this topic³²⁻³⁶. For instance, recent

advancements of near infra (NIR) C-dots and their biomedical applications have been systematically summarized by Xiong³⁷, and Qu's group³⁸. Reviews focused on one specific application of C-dots in biosensing^{39, 40}, phototherapy⁴¹, nanomedicine^{42, 43} as well as bone tissue engineering⁴⁴ have also been reported. Even though significant progress has been achieved, applications of CDs in biomedical fields still face some challenges. For instance, although enormous efforts have been devoted, majority of (NIR) CDs still suffered from relatively low PL quantum yields (QYs), significantly limiting their practical applications for bioimaging and theranostics development. Furthermore, the detection process of CDs in biosensing is often interfered by potential interferents due to the absence of specific recognition groups on surface of CDs for analytes; Most importantly, the interactions of CDs with biological systems are generally poor and lack specificity⁴⁵, significantly limiting their potential clinical applications.

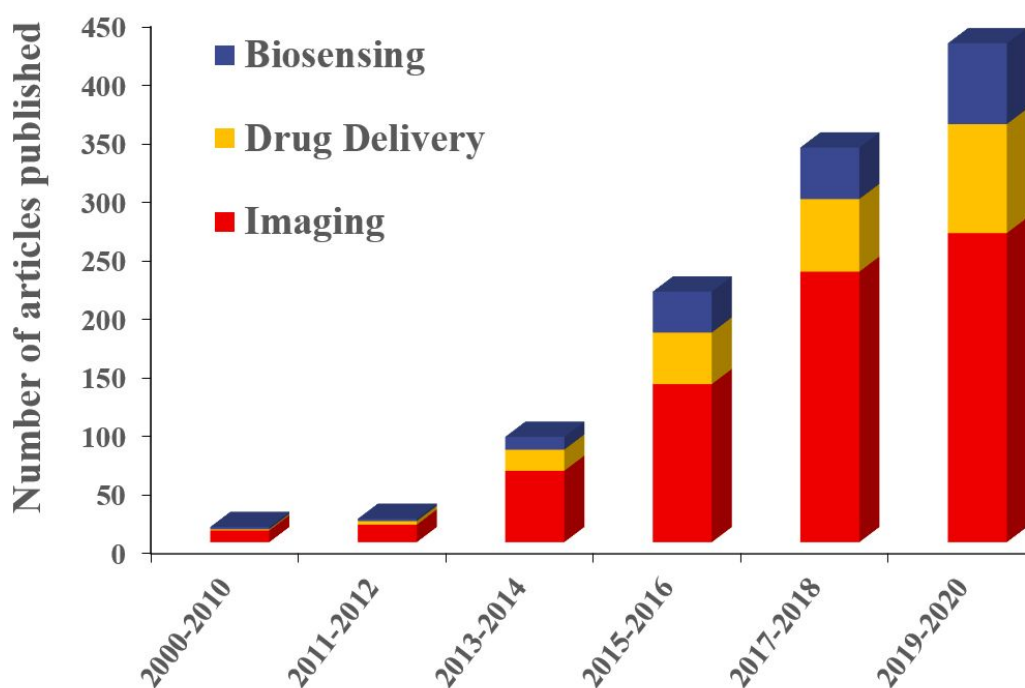


Figure 1. Number of articles published on the applications of CDs in biomedical fields, results obtained *via* Google Scholar on September 6th, 2021. Blue, yellow and red columns represent articles resulted from searching by the exact phases “carbon dots, carbon nano dots, carbon quantum dots, graphene quantum dots and C-dots” with “biosensing”, “drug delivery”, “imaging” occurring in the title of a paper, respectively.

CDs composites have turned out to be very successful in addressing the above-mentioned issues, and surface functionalization and heteroatom doping have proven to be among the most effective methods to obtain them^{46, 47}. Up to now, various traditional materials such as metals/metal oxides, nonmetallic inorganic materials as well as organics have been widely composited with CDs to enhance their intrinsic properties and expand their application scopes. In these systems, the merits are obvious by compositing CDs with traditional materials as regarding to their bioapplications. Firstly, the PLQYs of CDs could be generally increased by either compositing with metals and small organic molecules or *via* direct elements doping; furthermore, by properly tuning the compositing reagents, red shifting of the fluorescence emissions could be achieved for the resulted CDs composites compared to that of bare CDs. The enhancements in the PLQYs and red shift of the fluorescence emissions are extremely important for the further advancement of CDs in the biomedical fields. Secondly, CDs composites could be endowed some unique features that are highly advantageous for bioapplications but impossible to see in bare CDs. For instance, by compositing with ferromagnetic materials, CDs composites could be applied for dual mode (fluorescence and MRI) imaging, which is impossible to achieve in bare CDs. By compositing with metals or polymers, the mechanical strength of CDs could be greatly enhanced, which are rather important for their applications as scaffolds for bone tissue engineering. Thirdly, the composition of CDs with other molecules such as antibodies and nucleic acids could significantly enhance their sensitivity and specificity towards analytes, greatly expanding their application scope in biosensing. Lastly, the interactions of CDs with biological systems are generally lacking specificity, which limit their potential clinical applications. By compositing with proper molecular ligands, this shortcoming could be much alleviated. For instance, many reports have demonstrated that CDs could obtain high cancer targeting ability by functionalized with proper ligands. Indeed, studies have undoubtedly demonstrated the effectiveness of composites in improving the properties of CDs, enhancing their performances in various applications and expanding their application scopes^{48, 49}.

Despite the advancements, reviews specifically focus on CDs composites and their biomedical applications have been relative limited in literature. Currently, there are some summaries related to CDs composites, however, these reviews are generally sporadic and limited to a specific type of materials composited with CDs⁵⁰⁻⁵². Thus, a comprehensive review that specifically focuses on CDs composites and summarizes their biomedical applications systematically is still missing. In this context, this review aims to summarize the recent advancements in CDs composites syntheses and their applications in biomedical fields. Firstly, we will discuss the various materials that are composited with CDs, with an emphasis on their synthesis approaches. In this section, four types of CDs composites, namely metal-CDs, nonmetallic inorganics-CDs, organics-CDs, as well as multi-components-CDs composites, will be discussed in detail (**Figure 2**). Secondly, we will carefully discuss the biomedical applications of these CDs composites, including bioimaging, drug delivery and biosensing. Lastly, perspectives on the challenges and future trends of CDs composites will be provided.

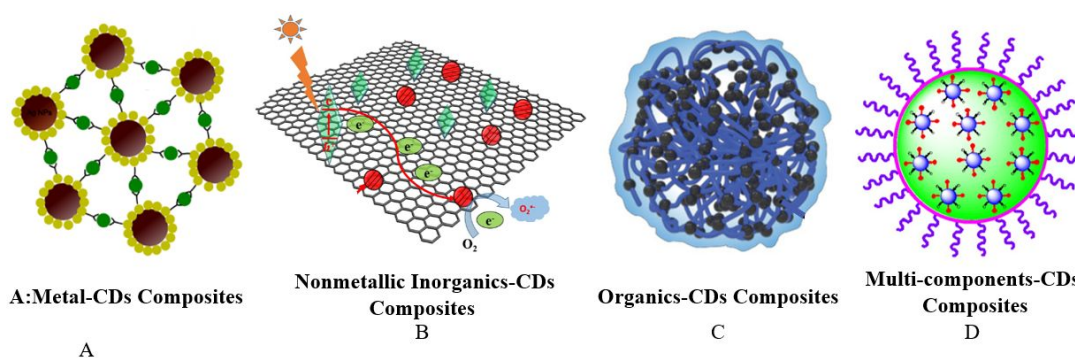


Figure 2. Cartoon representations of **A)** metal-CDs composites. Reproduced with permission from ref ⁵³. Copyright 2017, Elsevier. **B)** nonmetallic Inorganics-CDs composites. Reproduced with permission from ref ⁵⁴. Copyright 2016, Elsevier. **C)** organics-CDs composites. Reproduced with permission from ref ⁵⁵. Copyright 2019, WILEY - VCH. **D)** multi-components-CDs composites. Reproduced with permission from ref ⁵⁶. Copyright 2016, American Chemical Society.

2. Synthesis of CDs Composites

There are mainly three types of materials compounded with CDs, namely metals, nonmetallic inorganics and organics. Interestingly, syntheses for these CDs composites are very similar, and could be realized *via* physical mixing (i.e., stirring, ultrasonication), hydrothermal/solvothermal treatments, as well as microwave assisted treatments. Depending on the actual experiments undertaken, these methods can be regarded either as one-pot or stepwise approach. One-pot synthesis refers to reactions in which all the precursors are treated together, so that the syntheses of CDs as well as their composites with other materials are carried out all at once. This approach is relatively simple, cheap and efficient; however, it's generally suffered from inefficient control over the desired properties (i.e., size, surface chemistry, etc.) of the composites formed. On the other hand, in stepwise approach, CDs are prepared in advance, and follow-up reactions are generally required to compound them with other selected materials. This approach generally displayed a wider selection of components and behaves better in tuning the properties of the composites compared to one-pot approach.

2.1. Synthesis of Metal-CDs Composites

Metal-CDs composites are a major type of CDs-based composites and formed by composition of CDs with metals/metal oxides. Metals, including noble metals and transition metals, have been widely applied in optoelectronic, biomedicine and other fields because of their unique electrical and optical properties^{57, 58}. As a result, compositing metals with CDs to improve the photoelectric properties of CDs has attracted great attention⁵⁹⁻⁶¹. Depending on the structure of the composites formed, there are mainly three forms of metal presented in the metal-CDs composites, including metal ions/atoms, metal nanoparticles (MNPs) and metal oxides (MOs)⁶²⁻⁶⁵.

For the first type, it is generally regarded as metal ions/atoms doping, which not only improves the optical properties of CDs but also gives novel functionality to CDs

because of the modulation in the band structure. In most studies, composites of metal ions/atoms and CDs are mainly presented in the form of M@CDs and can be obtained through hydrothermal and chemical reductions^{66, 67} (**Figure 3A**). Strictly speaking, this type of composites is generally considered as metal-doped CDs, not CDs “composites”. On the other hand, MNPs are the most common forms in metal-CDs composites and they can be prepared *via* both physical (i.e., simple mixing and stirring) and chemical (i.e., reduction) means. In physical method, MNPs are generally prepared in advance, and they are normally formed through the reduction of metal ions *in situ* through chemical methods⁶⁸. MNPs and CDs are mainly compounded in the form of MNPs @ CDs (**Figure 3B**), however, sometimes they also form CDs@MNPs (**Figure 3C**) type of structures through covalent bonding⁶⁹⁻⁷¹. In addition, some of them can also form a core-shell structure (**Figure 3D**), in which MNPs function as the core, and CDs cover the surface to form the shell⁷². Lastly, MOs are also commonly recognized as important components in the metal-CDs composites and they generally form very uniform structures with CDs due to their excellent interactions with CDs⁷³ (**Figure 3E**). MOs-CDs composites are mainly prepared through hydrothermal/solvothermal treatments^{74, 75}. As can be seen, due to the presence of different forms of metals in the composites, as well as their different application purposes, synthesis methods for the preparations of metal-CDs composites are also quite diverse. Among the various methods, physical mixing, hydrothermal/solvothermal treatments and chemical reductions are the most frequently adopted approaches.

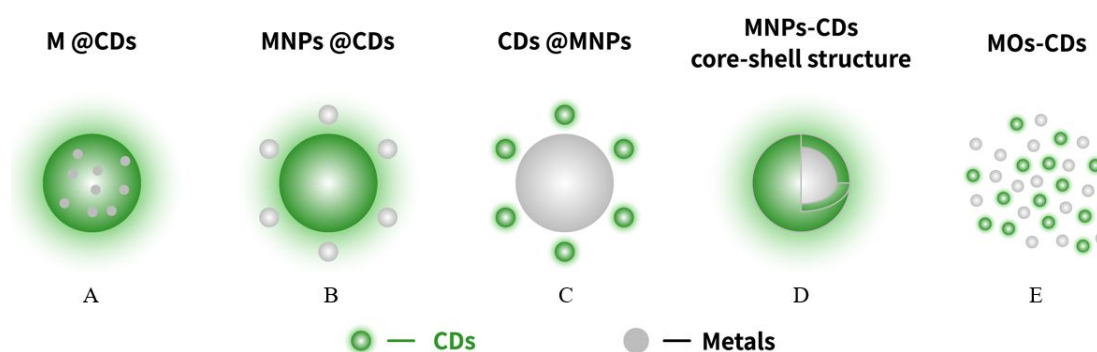


Figure 3. Cartoon representations of the possible structures of Metal-CDs composites, **A)** M@CDs, metal ions in the CDs; **B)** MNPs@CDs, metal nanoparticles on the surface of CDs; **C)** CDs@MNPs, CDs on the surface of metal nanoparticles; **D)** MNPs-CDs core-shell structure, metal nanoparticles as the core, CDs as the shell; **E)** MOs-CDs, metal oxides and CDs form uniform structures.

2.1.1. Synthesis *via* Physical Mixing

In this method, metal-CDs composites are prepared by mixing CDs solution with metal salt solution (or dispersions of MNPs), and the interactions of metals with CDs are generally facilitated by mechanical shearing, stirring and mixing, ultrasonic treatment as well as mild heating. This synthesis approach generally experiences very mild reaction conditions and is environment-friendly. However, the interactions of metals and CDs in the composites are normally poor⁷⁶. For instance, in a recent study, CDs were first synthesized *via* solvothermal treatment, then the as-prepared CDs were stirred with alkali metal solutions to generate the desired M@CDs composites⁷⁷. Interestingly, these metal-ion-functionalized CDs demonstrated excellent red-emissive PL properties with QYs of 34.09% (Li@CDs), 29.29% (Na@CDs) and 27.64% (K@CDs). The higher QY demonstrated by Li@CDs was attributed to the fact that Li atom exhibits higher electronegativity than Na and K. Unfortunately, the authors did not compare these composites with their counterparts, the metal-free CDs. Applying similar strategies, CDs were also composited with various MNPs (i.e., Au, Ag, and Pt) (**Figure 4A**)⁷⁸. In addition to metal atoms/ions and MNPs, the composites of CDs with MOs have also been achieved through physical mixing⁷⁹. As demonstrated, physical mixing is a facile method to prepare metal-CDs composites. However, it is worth noting that majority of metal-CDs composites are synthesized *via* other methods such as hydrothermal/solvothermal treatments, microwave-assisted method and electrochemical synthesis.

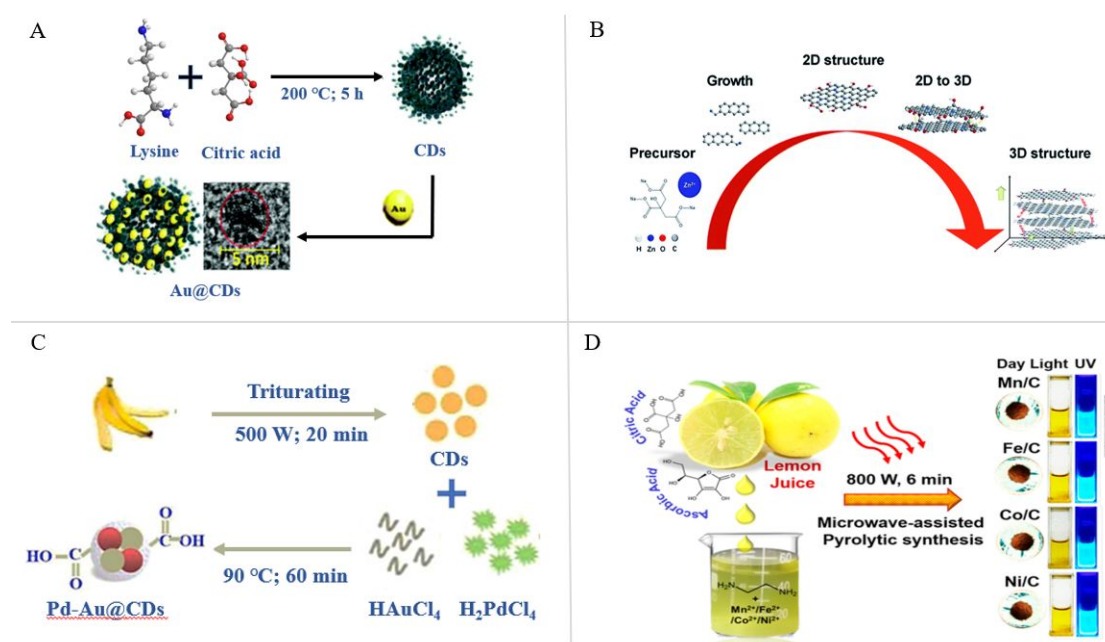


Figure 4. **A)** Schematic illustration of the synthesis process of Au@CDs. Reproduced with permission from ref⁷⁸. Copyright 2020, Royal Society of Chemistry. **B)** Schematic diagram showing the growth of the Zn-CDs from a sp^2 to a sp^3 structure. Reproduced with permission from ref⁸⁰. Copyright 2018, Royal Society of Chemistry. **C)** Schematic illustration of the synthesis process of Pd/Au-CDs. Reproduced with permission from ref^[61]. Copyright 2017, Elsevier. **D)** Schematic illustration of the synthesis process of metal ions (Mn^{2+} , Fe^{2+} , Co^{2+} , Ni^{2+})-doped CDs. Reproduced with permission from ref^[63]. Copyright 2018, American Chemical Society.

2.1.2. Synthesis *via* Hydrothermal / Solvothermal

Currently, hydrothermal treatment is the most widely used approach for preparations of metal-CDs composites. It is environment-friendly, easy to operate and has a unified reaction system; however, the reaction time could be long and reaction conditions are generally harsh (i.e., high temperature and pressure). Hydrothermal treatment could be used to obtain composites with controlled size, shape and establish strong interactions between the MNPs and CDs. Similarly, syntheses of metal-CDs composites *via* hydrothermal treatment could be broadly divided as one-pot and stepwise approach.

In the one-pot approach, the preparations of CDs and the composition with metals are achieved simultaneously in a one-pot fashion by mixing and treating the precursors of CDs and solutions of metal salts altogether. For example, Xu et al. synthesized

Zn@CDs using this one-pot hydrothermal treatment and the obtained composites demonstrated uniform sizes (3-10 nm) and bright blue fluorescence with QY >32%⁸¹. Interestingly, the same group demonstrated that the QY (35%) could be fine-tuned by manipulating the reaction time without affecting the morphologies of the composites (**Figure 4B**)⁸⁰. They attributed increase of the QY of the Zn-CDs to the reason that Zn could directly oxidize carbon-based surface passivation and prevent the aggregation of graphene π - π stacking. With the understanding towards the PL mechanism of metal-CDs composites, the same group further pushed their work in this area and successfully realized the synthesis of metal-CDs composite (Ba@CDs) with quantitative yield (99.6%). Unlike in the case of Zn-CDs, the authors attributed the high QY to the defected structures on CDs caused by the charge transfers from Ba atoms.⁸² In a different study, Cheng and co-workers realized a high QY of 51.2% on Zn-CDs composite, which they attributed to the radiative recombination of electrons and holes trapped on the CDs surface⁶⁷. As can be seen, the PL mechanisms for those metal-CDs composites with high QYs varied depending on the specific synthesis methods and compositing metals, which included increase of radiative pathways (i.e., surface states) of high QYs^{67, 82}, alleviating of fluorescence quenching⁸⁰, etc. With similar strategy, Cu²⁺@CDs and La@CDs have also been successfully prepared^{83, 84}. Stepwise approach refers to reactions in which CDs are prepared separately before they are treated hydrothermally with metals to generate the composites. For instance, Yu et al. successfully prepared TiO₂/CDs composite *via* hydrothermal treatment (140 °C for 4 h), in which the CDs were synthesized *via* an electrochemical treatment in advance⁸⁵.

Depends on the nature of the carbon precursor, as well as the purpose to control the particle size and shape of the composites, solvents other than water could be used. For example, Zhu et al. synthesized CDs-decorated NiCo₂O₄ nanohybrid by a two-step solvothermal method, in which ethylene glycol was used⁸⁶. Interestingly, in this stepwise approach, when composited with noble metals (NMs), CDs tend to deposit onto the surfaces of NMs, forming “CDs@MNPs” type structures (**Figure 3C**)⁸⁷. The

composites of CDs with NMs (i.e., Au, Ag, Pt) are generally mutual-beneficial: firstly, during synthesis of NMs/CDs nanohybrids, CDs with abundant oxygen-containing functional groups (i.e., carboxyl and hydroxyl groups) could prevent NMs from aggregation and ensure the activity of NMs by engineering the properties (i.e., sizes) of NMs^{88, 89}. Secondly, the hybridized NMs also facilitate the realization of high dispersibility of CDs. Most notably, the superior electronic properties of both CDs and NMs can facilitate electrons transfer, resulting the restriction of charge carrier recombination by ultrafast relaxation process of localized surface plasmon resonance (LSPR) induced hot electrons⁹⁰, which can boost the performances toward more effective environmental sensing, pollutants treatment and energy conversion^{91, 92}.

2.1.3. Synthesis *via* Chemical Reduction

Chemical reduction is a conventional method for the syntheses of metal-CDs composites, which refers to the preparation of metal-CDs composites by reducing metal precursors to MNPs and then compounding with CDs. For instance, Huang et al. synthesized Au@CDs by reducing HAuCl₄ with sodium citrate, and then mixed with CDs at 100 °C for 80 min⁹³. With similar strategy, Liu and co-workers prepared CDs which could be adsorbed on surface of AuNPs through electrostatic interaction⁹⁴. In these syntheses, commonly used reductants for the reduction of metal ions include boron hydride, sodium citrate and etc.⁹³⁻⁹⁵. However, these metal reductants belong to dangerous chemicals and are easy to introduce by-products during synthesis, thus the preparations of metal-CDs composites without these traditional reductants are greatly desired.

Considering the fact that there are generally rich reducing functionalities (i.e., amines, alkenes, etc.) on CDs, it might be possible to use CDs separately and directly to reduce metal ions by accelerating electrons transfer and stabilize the formed MNPs. Indeed, studies have demonstrated the possibility of using CDs as reductants in the preparations of MNPs-CDs composites⁹⁶. Depending on the nature of the CDs used, the reaction conditions for the reduction of metals can vary significantly. For example,

to prepare AuNPs–CDs core–shell nanocomposites, Sonam et al. mixed HAuCl_4 solution and CDs at room temperature; while Luo and co-workers applied a much harsher condition (100 °C). In these two examples, CDs were synthesized by microwave irradiation and electrochemical method, respectively^{97, 98}. Interestingly, the QY of AuNPs-CDs composite was only 0.5% in Luo's study, the extremely low QY was attributed to the quenching effect rising from the photoinduced electron transfer from CD shells to Au cores and the nucleation of CDs⁹⁹. In addition to the composition with single NMs, Huang and co-workers also reported the composition of Pd and Au with CDs, the composite (Pd-Au@CDs) demonstrated a relatively higher QY of 16% (**Figure 4C**)¹⁰⁰. Inspired by these studies, Ag-CDs nanocomposites have also been reported¹⁰¹.

Generally speaking, noble metal ions tend to accumulate onto the surface of CDs owing to the rich presence of oxygen-containing groups during chemical reductions; this process could promote the formation of noble MNPs, leading to a reverse core-shell structures (see **Figure 3D**, where CDs as core, and MNPs as shell instead). This technique has the advantage of short preparation time and simple reaction conditions (i.e., room temperature and atmospheric pressure), however, it could be difficult to control the size of MNPs and it might potentially pollute the environment.

2.1.4. Synthesis *via* Other Preparation Methods

In addition to the above-mentioned methods, some other preparation methods such as microwave-assisted synthesis and sonochemical method are commonly used. For instance, Sajid et al. reported ethylenediamine-functionalized transition metal ion-doped CDs by microwave-assisted pyrolysis at 800 W for 6 min. Compared to the QY of the pristine CDs (48.31%), the synthesized Mn^{2+} @CDs, Fe^{2+} @CDs, Co^{2+} @CDs, Ni^{2+} @CDs exhibited QYs of 35.71, 41.72, 75.07, and 50.84%, respectively. The authors suggested that the enhancement or quenching of PL depended on the interactions of transition-metal ions that acted as dopants with the surface of CDs. The Co^{2+} @CDs presented the highest QY, which was attributed to the

fact that Co^{2+} prevented the formation of complexes and the secondary amine moieties were bound to primary oxy-functional groups on the surface emissive trap sites of CDs (**Figure 4D**)¹⁰². In a different study, Vijay et al. reported a one-step sonochemical synthesis of a series of CDs from PEG with five different metals (Ag, Au, Ga, Sn and Zn) that were yellow to brownish-red in color with the highest QY reaching 16%¹⁰³. In addition to these preparation methods, carbonization under high temperature have also been used to prepare $\text{Eu}^{3+}@$ CDs¹⁰⁴. In summary, metal-CDs composites have increasingly attracted more attention in recent years and many studies regarding the synthesis, properties and applications of this type of composite have been reported. Selective examples of metal-CDs composites systems have been summarized in **Table 1**.

Table 1. Selective examples for the synthesis of metal-CDs composites

Composite Form	Carbon Source ^{d)}	Synthesis Method ^{e)}	Reaction Parameters	Size (nm)	QY (%) ^{f)}	Application	Ref.
Li@CDs	CA; urea	PM	1/60 h	3-5	34.09	pH sensing	77
Au@CDs	CA; Lys	PM	37 °C, 1/3 h	3.9-4.7	-	Colorimetric sensing	78
Zn@CDs	SC	Hydrothermal	185 °C, 1-10 h	3-10	34.6	Biosensor	80
$\text{Cu}^{2+}@$ CDs	Tea	Hydrothermal	150°C, 6h	-0.85	3.26	Nanoprobe	83
La@CDs	ATP	Hydrothermal	160 °C, 8 h	3.97-4.64	13.9	Biosensor, bioimaging	84
TiO ₂ /CDs	Graphite	Hydrothermal	140 °C, 4 h	20-30	-	Photocatalytic	85
CDs-MOs ^{a)}	Graphite	Solvothermal	180 °C, 3 h	250-350	-	Supercapacitor	86
Pd/Au-CDs	BP	CR	90 °C, 1 h	5-15	16	Biosensor	100
M@CDs ^{b)}	CLE	Microwave	800 W, 1/10 h	2.72-3.69	35.71-75.07	Bioimaging	102
M@CDs ^{c)}	PEG	Sonochemical	3 h	6-8	1.8-16	Cell labeling	103
Ag@CDs	GR	PM	1/2 min	~4	-	Immunosensor	105

CDs@Pt	LasA	PM	48 h	~10	-	Biosensor	106
--------	------	----	------	-----	---	-----------	-----

-
- a) MOs = NiCo₂O₄;
- b) M = Mn, Fe, Co and Ni;
- c) M = Ga, Sn, Zn, Ag and Au;
- d) CA: citric acid; Lys: L-lysine; GR: graphite rod; LasA: L-ascorbic acid; SC: sodium citrate; ATP: adenosine disodium triphosphate; BP: banana peels; CLE: citrus lemon extract; PEG: polyethylene glycol;
- e) PM: physical mixing; CR: chemical reduction;
- f) QY: quantum yield.

2.2. Synthesis of Nonmetallic Inorganics-CDs Composites

Nonmetallic inorganics-CDs composites are another type of composites derived from CDs by compositing with inorganic materials such as ceramics^{107, 108}, quantum dots (QDs)¹⁰⁹, graphene¹¹⁰ as well as carbon nanotubes (CNTs)^{111, 112}. Precisely speaking, metals (including metal nanoparticles and metal oxides) as well as the above-mentioned materials (ceramics, QDs, graphene and CNTs) could all be classified as inorganics. Since there have been enormous studies on metal-CDs composites, and the optical properties tuning, application scopes of metal-CDs composites are quite different from other nonmetallic inorganics-CDs composites, thus we departed a separate section for metal-CDs composites, which were discussed above. As such, in this section, we will specifically focus on the nonmetallic inorganics-CDs composites that involved the above-mentioned traditional inorganic materials.

2.2.1. Synthesis of Nonmetallic Inorganics-CDs Composites by Heteroatom Doping

Strictly speaking, heteroatom doping of CDs is hardly to be considered as “composites” of CDs with inorganic materials, however, there have been much work on heteroatom doping of CDs^{113, 114}, which was very effective in enhancing the properties of CDs. Therefore, we dedicated a short section to discuss heteroatom doping and their effects on CDs composites. Heteroatom doping can be divided into

single atom doping and multiple atoms co-doping. There have been many reports about single-atom doped CDs, including nitrogen¹¹⁵, sulfur¹¹⁶, boron¹¹⁷, phosphorus¹¹⁸, silicon^{119, 120} and fluorine¹²¹. By introducing atomic impurities into CDs, their electronic structures could be adjusted to generate n- or p-type carriers. As a result, the electronic and optical properties of CDs could be fine-tuned by using specific doping atoms. Single atom doping exhibits great potential in tuning the intrinsic properties of CDs, however, it also has limitations. One of the major limitations is that the emission spectra is generally confined to single atom doped CDs. Therefore, doping of CDs with multiple atoms has attracted much attention, since it could create unique electronic structures due to the synergistic effects from the various doped heteroatoms in CDs¹⁸. Up till now, co-doping of CDs with N/S¹²²⁻¹²⁵, N/P¹²⁶, N/B^{127, 128}, N/S/B¹²⁹ and N/S/P^{130, 131} have all been reported.

2.2.2. Synthesis of Nonmetallic Inorganics-CDs Composites by Compositing with Traditional Inorganic Materials

Depending on the nature of the inorganic molecules, the nonmetallic inorganics-CDs composites could be prepared *via* physical mixing, hydrothermal treatment^{132, 133}, sol-gel method and microwave radiation¹³⁴⁻¹³⁷.

2.2.2.1. Synthesis *via* Physical Mixing

As one of the most widely used ceramic materials, alumina (Al_2O_3) is often used as adsorbent, catalyst and sensor material because of its large surface area, high thermal stability and good mechanical strength^{138, 139}. Composites of alumina and CDs have been shown to prevent aggregations and improve thermal stability of CDs; endow alumina with better PL properties, improving its applications in the optoelectronic fields. In most studies, CDs and mesoporous aluminas (MAs) were prepared individually in advance, and then the two were assembled *via* hydrogen-bonding interactions under simple stirring (**Figure 5A**)^{140, 141}. In another study, the MAs-CDs composites, which were prepared through the same method, demonstrated much

higher fluorescence QY (46.69%) and long-term stability, while the QY of CDs were ~33% and the QY of MAs were ~2.11% (Figure 5B)¹⁴².

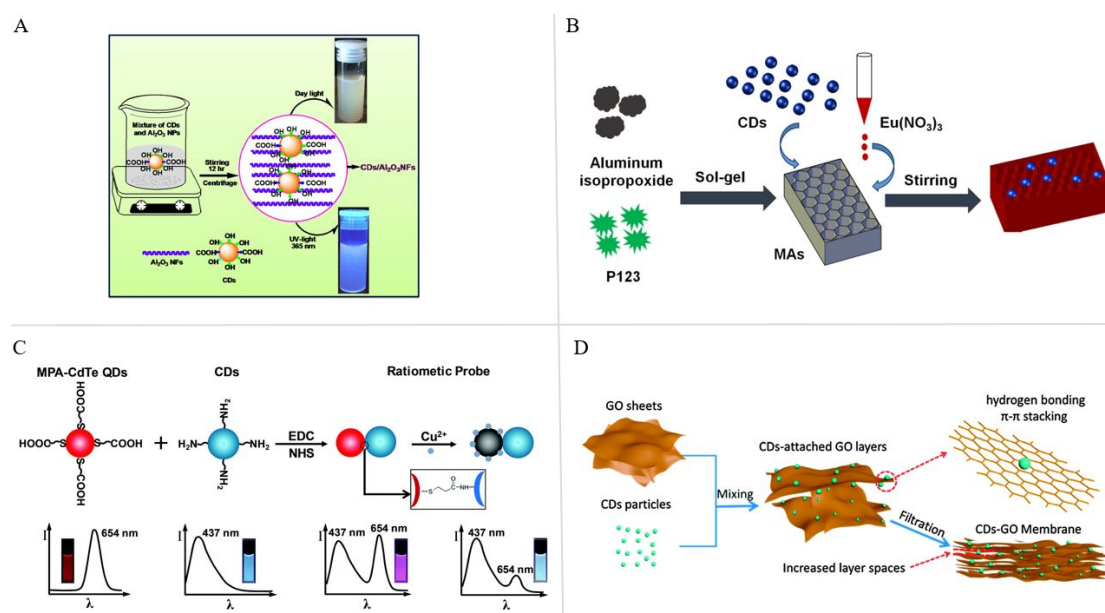


Figure 5. **A)** Schematic illustration of the synthesis process of CDs/Al₂O₃NFs. Reproduced with permission from ref ¹⁴⁰. Copyright 2020, Elsevier. **B)** Schematic illustration of the synthesis process of CDs/MAs hybrid materials. Reproduced with permission from ref ¹⁴². Copyright 2017, Elsevier. **C)** Schematic illustration for the synthesis of composite derived from carboxyl-modified red fluorescent cadmium telluride (CdTe) quantum dots and amino-functionalized CDs for the determination of Cu²⁺. Reproduced with permission from ref ¹⁴³. Copyright 2016, Royal Society of Chemistry. **D)** Schematic illustration of the fabrication process of CDs–GO membranes. Reproduced with permission from ref ¹⁴⁴. Copyright 2014, Royal Society of Chemistry.

QDs derived from semiconductors have attracted much attention in the optoelectronic field because of their unique electronic and optical properties, such as high extinction coefficient, high fluorescence quantum efficiency, size-dependent broad absorption, and excellent photochemical stability¹⁴⁵⁻¹⁴⁷. Recently, they have been composited with CDs to achieve unique properties. For instance, a ratiometric fluorescence sensor was prepared *via* simple mixing and stirring of CDs and QDs for the detection of Hg²⁺ and Cu²⁺ (Figure 5C)¹⁴⁸. In addition to the above-mentioned examples, CNTs, SiO₂ and GO have also been composited with CDs *via* simple physical mixing (Figure 5D)¹⁴⁹⁻¹⁵¹.

2.2.2.2. Synthesis *via* Hydrothermal/Solvothermal

Hydroxyapatite (HAp) is a natural mineral form of calcium apatite and the main inorganic components of bone tissues. HAp exhibits good biocompatibility and bone bioactivity, thus is widely used as scaffolds in bone tissue engineering (BTE)^{152, 153}. Recently, much attention has been paid to the composites of HAp and CDs for the application in the biomedical field, more specifically, BTE¹⁵⁴⁻¹⁵⁶. Composites of HAp and CDs are mainly prepared *via* hydrothermal treatment, which could produce composites with uniform structures, controlled sizes and strong interactions between HAp and CDs. Depending on the nature of the precursors, the synthesis of the composites could be prepared *via* four different routes: 1) raw materials of HAp and carbon precursors are treated hydrothermally in a one-pot fashion, and the formation of HAp, CDs as well as their composites are achieved simultaneously (**Figure 6A**)^{157, 158}; 2) HAp is pre-synthesized or readily-made, and then treated hydrothermally with carbon precursors; 3) CDs are pre-synthesized, and then treated hydrothermally with raw materials of HAp¹⁵⁹; 4) both HAp and CDs are synthesized in advance, and then the two are treated together hydrothermally to obtain their composites¹⁶⁰. In addition to HAp, the composites of CDs with other bioceramics (i.e., Si, SiO₂) could also be achieved *via* simple hydrothermal treatment of the two components^{161, 162}.

Graphene and its derivatives (i.e., graphene oxide) have good physical and chemical properties, however, due to their strong π - π stacking and van der Waals interaction among the sheets, it's common to observe irreversible agglomeration and precipitation in their aqueous solutions, significantly limiting their practical applications^{163, 164}. Encouragingly, by compositing with CDs, the aggregations of graphene and its derivatives could be effectively prevented, probably due to the insertions of CDs between the sheets. As a result, their practical applications in the biomedical fields are greatly improved¹⁶⁵. What's more, CDs can function as reducing agents during the composite process, generating CDs-reduced graphene oxide (rGO) composites. The CDs/rGO hybrids have been demonstrated as efficient probes for the detection of dopamine and acetylcholine, as well as electrocatalysts for

electrochemical energy conversion¹⁶⁶⁻¹⁶⁹. In a different study, Yang et al. synthesized NH_4F -CDs composite using citric acid, thiourea and ammonium fluoride by a solvothermal method¹⁷⁰, in which the emissions of the composite were pushed to the NIR region by the negatively charged, electron-withdrawing F^- which could reduce the bandgap. In addition to these examples, the composites of CDs with other inorganic materials such as NH_2 , TiO_2/GO , $\text{HAp}/\text{Ag}_3\text{PO}_4$ have also been reported (**Figure 6B**)^{171, 172}.

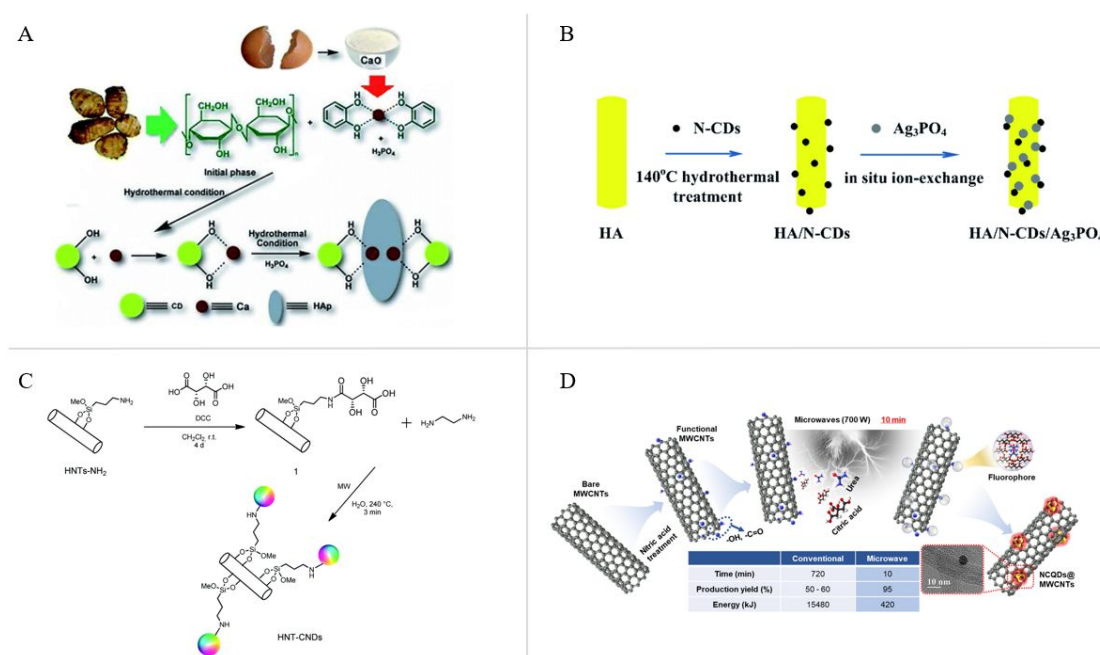


Figure 6. **A)** Schematic illustration of the synthesis process of CD@HAp nanohybrid. Reproduced with permission from ref¹⁵⁸. Copyright 2016, Royal Society of Chemistry. **B)** Schematic illustration of the synthesis process of $\text{HA/N-CDs/Ag}_3\text{PO}_4$. Reproduced with permission from ref¹⁷². Copyright 2017, Royal Society of Chemistry. **C)** Schematic illustration of the synthesis process of HNT-CDs . Reproduced with permission from ref¹⁷³. Copyright 2018, Royal Society of Chemistry. **D)** Schematic illustration of the synthesis process of NCQDs@MWCNTs . Reproduced with permission from ref¹⁷⁴. Copyright 2020, Elsevier.

2.2.2.3. Synthesis *via* Other Preparation Methods

In addition to physical mixing and hydrothermal treatment as mentioned above, there are also some other methods (i.e., microwave-assisted synthesis) for the composition of CDs with inorganic materials. Microwave-assisted synthesis is an augmentation to the solvothermal/hydrothermal technique where microwave is utilized instead of

heat¹⁷⁵. Compared to hydrothermal treatment, it has the advantages of short preparation time, environment-friendly and low cost. For example, Marina et al. synthesized fluorescent halloysite nanotubes (HNTs) by the direct covalent linkage of CDs on the halloysite external surface (**Figure 6C**)¹⁷³. In another study, CDs were shown to grow on MWCNTs *via* an one-step microwave-assisted treatment, and the composites turned out to be promising electrocatalysts (**Figure 6D**)¹⁷⁴. In addition to microwave-assisted method, there were reports showing that CDs@SiO₂ nano phosphors were synthesized by reversed-phase microemulsion method and Si-CDs/SiO₂ nanocomposites were generated through a calcination process^{176, 177}. Selective examples of nonmetallic inorganics-CDs composites systems have been summarized in **Table 2**.

Table 2. Selective examples for the synthesis of nonmetallic inorganics-CDs composites

Composite Form ^{a)}	Carbon Source ^{b)}	Synthesis Method ^{c)}	Reaction Parameters	Size (nm)	QY (%) ^{d)}	Application	Ref.
CDs/MAs	EDA	PM	8 h	/	46.69	TP	142
CQD@f-MWCNTs	AC	PM	4 h	10-50	/	ES	150
CDs-SiO ₂	CA	PM	80 °C, 3 h	84-190	34	Sensor	178
NCQDs/HAp	CA	Hydrothermal	190 °C, 24 h	30-200	31.43	/	157
CD@HAp	CCE	Hydrothermal	170 °C, 15 h	50-80	/	BTE	158
Si-CDs	Tri-SC	Hydrothermal	200 °C, 2 h	3-7	30	Biosensor	161
CDs-SiO ₂	APTMS	Hydrothermal	300 °C, 2 h	1-5	42.6	TP	162
CDs@rGO	GO	Hydrothermal	300 °C, 2 h	/	/	Biosensor	166
rGO-CDs	Sucrose	Hydrothermal	90 °C, 4 h	5-15	/	Biosensor	167
HNT-CDs	TTA	Microwave	200 W, 1/20 h	3.3-4.7	17	/	173
CQDs@SiO ₂	CA	RPMM	/	18-159	/	LED	176

^{a)} MAs: mesoporous aluminas; f-MWCNTs: functionalized multi-walled carbon nano tubes; HAp: hydroxyapatite; rGO: reduced graphene oxide; HNT: halloysite;

- b) EDA: ethylenediamine; AC: activated carbon; CA: citric acid; CCE: corms of *Colocasia esculenta*; GO: graphene oxide; Tri-SC: trisodium citrate; APTMS: 3-aminopropyltrimethoxy-silane; APBA:3-aminophenylboronic acid; TTA: tartaric acid;
- c) PM: physical mixing; RPMM: reversed-phase microemulsion;
- d) QY: quantum yield.
- e) TP: Temperature probes; ES: Electrochemical sensor; BTE: bone tissue engineering; LED: light-emitting diodes.

2.3. Synthesis of Organics-CDs Composites

Organic materials utilized to compound with CDs include small organic molecules (i.e., folic acid), organic dyes (i.e., Rhodamine B), gels and polymers. Among them, polymers have been the mostly applied organic molecules for compositing with CDs. Compounding CDs with polymers not only enhance the performance of the polymers (i.e., improvising the flexibility, strength, durability, and hydrophilicity)¹⁷⁹, but also passivate surfaces of CDs to enhance their PL intensity and the optoelectronic properties¹⁸⁰. There are generally three types in which polymers were used in the preparations of CDs: polymers as direct precursors for CDs synthesis, polymers as indirect precursors for CDs synthesis, and polymers for CDs surface modifications⁵¹. And the last aspect, polymers for CDs surface modifications/passivations, will be focused on in this section.

2.3.1. Synthesis *via* Physical Stirring

Physical stirring technique is normally used in stepwise synthesis strategy, in which CDs are synthesized in advance before compounding with organics. Stepwise approach for the preparation of organics-CDs composites has received significant attention due to its wide applicability and good compounding effects. For instance, modifications with polyethylenimine (PEI) can improve the PL property and biocompatibility of CDs, since the amino groups of PEI can generate strong hydrogen bonding with organic compounds containing oxygen- or nitrogen-functional groups. In another example, Han and co-workers synthesized PEI-CDs by simply stirring the mixture of PEI and CDs, and the obtained composite had a QY of 3.5%^{181, 182}. In addition to polymers, small nitrogen-containing organic molecules such as 2,2'

-(ethylenedioxy)bis(ethylamine) (EDA) was also commonly used to passivate CDs, which could enhance the optical properties (**Figure 7A**)¹⁸³. In these compositions under physical stirring, the forces that are responsible for the interactions of CDs and organic molecules were quite different. For instance, in Wu and co-workers' report, negatively charged CDs interacted with tetraplatinated porphyrin (PtPor) to form composite *via* electrostatic forces¹⁸⁴. While in another study, CDs-aggregation-induced emission (AIE) composite was formed through supramolecular assembling of CDs and hydrophobic AIEgen¹⁸⁵. In some studies, CDs and organic molecules could be composited *via* covalent bonding under very mild conditions (i.e., stirring at r.t.). For example, RhB-CDs composite was obtained by mixing the solutions of activated CDs and RhB, in which the amino groups of RhB covalently reacted with the carboxyl groups on the CD surface¹⁸⁶. Similarly, CDs could be facilely conjugated with folic acid (FA) *via* simple crosslinking chemistry^{187, 188}. The compositions of CDs with these organic molecules were extremely useful in enhancing the optical properties of CDs and endowing them with unique properties (i.e., cancer targeting ability).

2.3.2. Synthesis *via* Hydrothermal/Solvothermal

Considering its environment-friendliness and strategy-convenience, hydrothermal treatment is also generally used for the composites of organics and CDs, either *via* one-pot or stepwise synthesis. Polyethylene glycol (PEG) has been widely applied to compound with CDs since a skin layer of PEG may increase the biocompatibility, enhance photostability, and even cause red-shifting in fluorescence emission of CDs¹⁸⁹⁻¹⁹². To study the effects of CDs and PEG on the properties of the obtained composites, some research groups have synthesized a series of CDs using different precursors (i.e., TNP, chitosan) with the same preparation method but different reaction conditions, and composited these CDs with PEG.¹⁹³

Besides PEG, hydrothermally-prepared PEI-CDs composites were also frequently reported (**Figure 7B**)¹⁹⁴. For instance, Dong et al. synthesized branched

polyethylenimine (BPEI)-CDs through the low temperature carbonization method. The obtained BPEI-CDs exhibited strong FL activity with a high PL QY (42.5%)¹⁹⁵. Interestingly, in some of these studies it was observed that fluorescence intensity of PEI-CDs decreased with the increase of solution pH, and thus could be used to develop pH sensors¹⁹⁶. In addition to these examples, other organics-CDs composites such as (N-(2-aminoethyl)-3-aminopropyl)tris-(2-ethoxy) silane-CDs(KH791-CDs), N-isopropylacrylamide-CDs(NIPAAM-CDs), CDs-RhB core-shell nanocomposite and (polyamidoamine)-PAMAM-NH₂-CDs have also been reported¹⁹⁷⁻²⁰⁰. It's also worth to mention that the QY of NIPAAM-CDs was as high as 94%. Interestingly, in hydrothermal reactions, the solvents used for work-up could play important roles. For instance, Lu and co-workers prepared dopamine-CDs composites through one-pot hydrothermal method and the resulted composites were extracted with two different solvents (water and ethanol). Surprisingly, the two dopamine-CDs composites exhibited different physical (i.e., solubility) and optical properties, the emission of dopamine-CDs composite extracted from ethanol was centered at 710 nm with QY of 26.28%, while that of composite extracted from water was centered at 685 nm with a higher QY (33.96%)^{201, 202}.

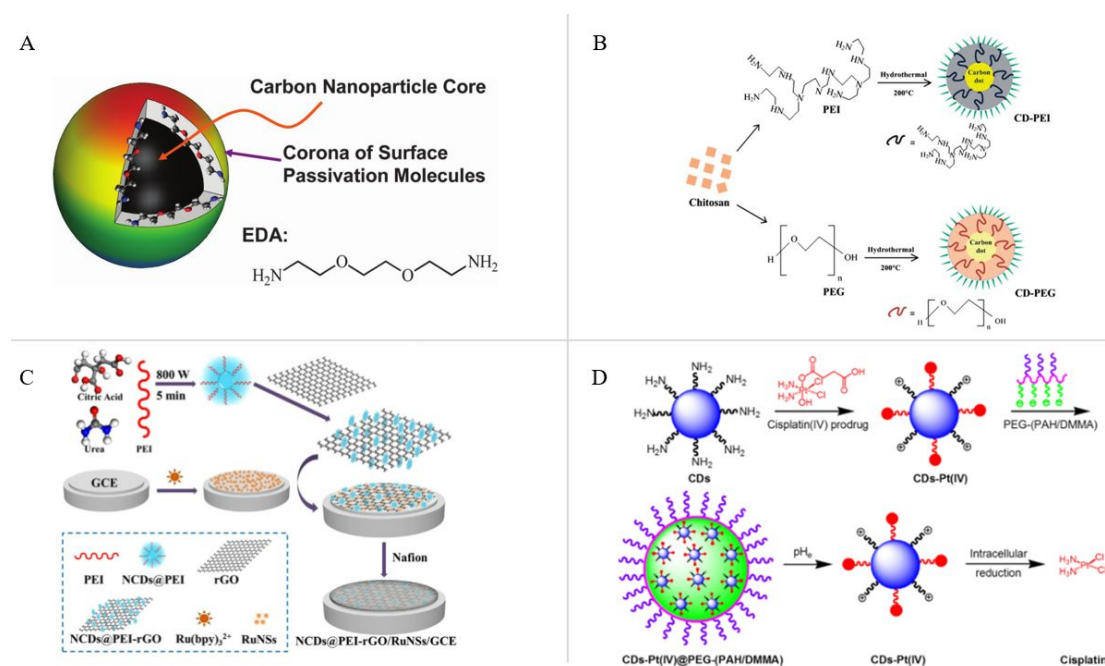


Figure 7. **A)** A cartoon showing the core-shell structure of EDA-CDs. Reproduced with permission from ref ¹⁸³. Copyright 2016, Royal Society of Chemistry. **B)** Schematic illustration of the synthesis process of CD-PEI and CD-PEG. Reproduced with permission from ref ¹⁹⁴. Copyright 2014, Royal Society of Chemistry. **C)** Schematic illustration of the construction process for PEI-N-CDs based ECL biosensor. Reproduced with permission from ref ²⁰³. Copyright 2016, Elsevier. **D)** Schematic illustration of the synthesis process of CDs-Pt (IV)@PEG-(PAH/DMMA). Reproduced with permission from ref ⁵⁶. Copyright 2016, American Chemical Society.

2.3.3. Synthesis *via* Microwave-assisted Treatment

Microwave-assisted synthesis is widely used in the preparation of organics-CDs composites due to its short reaction time and low cost. Since microwave irradiation can provide high energy in very short duration, the selection of a suitable reaction time is essential for tuning the properties of the composites formed. For instance, Liu and co-workers synthesized PEI-CDs *via* microwave-assisted treatment and only a specific microwave pyrolysis condition (700 W for 15 min) could result in excellent PL performance: shorter irradiation time led to incomplete surface passivation, while longer time led to the formation of large particles, both of which resulted low PL^{204, 205}. In a different study, RNase A@CDs composite with QY of 24.2% was also prepared *via* microwave-assisted treatment²⁰⁶. Selective examples of organics-CDs composites have been summarized in **Table 3**.

Table 3. Selective examples for the synthesis of organics-CDs composites

Composite Form ^{a)}	Carbon Source ^{b)}	Synthesis Method	Reaction Parameters ^{c)}	Size (nm)	QY (%) ^{d)}	Application	Ref.
EDA-CDs	CNP	Stirring	120 °C, 72 h	~5	15-20	Composite films	183
CDs@PtPor	CA	Stirring	R.T, 24h	6~9	36	Cancer therapy	184
FA-CDs	Dandelion leaf	Stirring	R.T, 24h	5~8	/	Bioimaging	187
PEG ₆₀₀₀ -CDs	TNP	Hydrothermal	180 °C, 12 h	51-120	/	Bioimaging	193
BPEI-CQDs	CA	Pyrolysis	<200 °C, 1/3 h	4-10	42.5	Chemical	195

							sensor	
PEI-CDs	EG, PEI	Hydrothermal	180 °C, 24 h	6-10	38	Fluorescence probe	196	
KH791-CDs	LasA	Hydrothermal	92 °C, 12h	3-4	8.6	Solar cells	197	
NIPAAAM-CDs	CA	Hydrothermal	160/200°C, 5 h	2-3	94	Bioimaging	198	
							Gene	
PEI-CDs	Glycerol	Microwave	700W, 1/12-1/4 h	3-13	7-15.3	delivery, bioimaging	204	
RNase A-CDs	CA	Microwave	700 W, 1/15 h	25-45	24.2	Bioimaging	206	

a) BPEI: branched polyethylenimine; EDA: 2,2'-(ethylenedioxy)bis(ethylamine); PtPor: tetraplatinated porphyrin; FA: folic acid; PEG₆₀₀₀: polyethylene glycol 6000; PEI: polyethylenimine; KH791: (N-(2-aminoethyl)-3-aminopropyl)tris-(2-ethoxy) silane; NIPAAAM: N-isopropylacrylamide; RNase A: ribonuclease A;

b) CA: citric acid; CNP: carbon nano powder; TNP: 1,3, 6-trinitropyrene; EG: ethylene glycol; PEI: polyethylenimine; LasA: L-ascorbic acid;

c) R.T: room temperature

d) QY: quantum yield.

2.4. Synthesis of Multi-Components-CDs Composites

Multi-components-CDs composites refer to two or more different types of materials composited with CDs. Compared to single-component-CDs composites, multi-components-CDs composites generally demonstrate better performances (i.e., enhanced fluorescence properties, increased QYs, and expanded application scopes)²⁰⁷⁻²⁰⁹. For example, study showed that Mg-CDs and EDA-CDs composites had QYs of 18.2 and 73.1%, respectively; however, the multi-components composite Mg-EDA-CDs presented a much higher QY than the two, reaching 83.0%²¹⁰. Despite multi-components-CDs composites bear superior properties; they come with some indelible shortcomings: 1) due to the involvement of multi components, the preparations of multi-components-CDs composites are much more complicated compared to those of single-component-CDs composites^{211, 212}. 2) The characterizations of multi-components-CDs composites are also much more challenging, and spectra are generally more complex²¹³⁻²¹⁵. As a result, studies

reported so far regarding multi-components-CDs composites fabrications are generally focusing on the doping effects of different elements from these components composited with CDs.

2.4.1. Synthesis *via* Hydrothermal/Solvothermal

By compounding with more than one type of materials, various elements (atoms) could be introduced into CDs, which can endow CDs with excellent properties (i.e., high QYs, wide emission). Thus, multi-atoms co-doping composites have attracted significant attention. Among the elements, N is the most commonly used dopant considering its comparable size and the ability to form strong bonds with carbon. On the other side, chelation of metal ions are conducive to the combination of amino and carboxyl groups on CDs through chemical reaction procedures, thus N- and metal ions-containing materials are commonly composited with CDs²¹⁶. Most of these composites can be achieved *via* simple hydrothermal treatment, for instance, Au, N-CDs; Ag, N-CDs; Cu, N-CDs; Al, N-CDs and Mg, N-CDs composites have all been reported, in which Mg, N-CDs demonstrated the highest QY of 58.8%²¹⁷⁻²²¹. Interestingly, the coordination bonds between silver ion and nitrogen atom can enlarge the band gap of CDs, resulting in enhanced fluorescence emission²²². In addition to these examples, Fe, Br-CDs and N, S-CDs-MnO₂ nano-composites have also been synthesized through simple hydrothermal treatments^{223, 224}.

2.4.2. Synthesis *via* Microwave-assisted Treatment

Known for short preparation time and simple procedures, microwave-assisted synthesis is also commonly applied for the preparation of multi-components-CDs composites. For instance, Sai et. al. successfully synthesized nitrogen and zinc co-doped CDs (N, Zn-CDs) with microwave-assisted treatment (130 °C for 60 min). Interestingly, the N, Zn-CDs exhibited bluish-green luminescence with a high QY (74%), while control sample (N-CDs) displayed blue luminescence with a much lower QY (2.63%). Authors attributed this phenomenon to the presence of oxygen

functionalities in the ZnO lattice structure, which might have lowered the energy required for the electronic transitions responsible of the radiations²²⁵. In addition, synthesis of PEI-N-CDs²⁰³ (**Figure 7C**) and N,S-CDs-P25²²⁶ hetero structural nanocomposites *via* microwave-assisted treatments have also been reported.

2.4.3. Synthesis *via* Other Preparation Methods

In addition to hydrothermal- and microwave-assisted synthesis, some other approaches such as physical stirring, ultrasound, chemical coupling have also been reported for the composites of CDs with more than one type of components²²⁷. In these approaches, however, it generally requires a separate step to prepare CDs in advance, following which the obtained CDs can be then compounded with other components. For instance, Deng et al. prepared a N-CDs-AuNPs nanosensor by assembling the N-doped CDs shell on AuNPs²²⁸. Tao et. al. reported a CDs-Pt(IV)@PEG-(PAH/DMMA) composite which was based on cisplatin(IV) prodrug-loaded charge-convertible CDs (**Figure 7D**)⁵⁶.

3. CDs Composites for Biomedical Applications

3.1. CDs Composites for Bioimaging

Considering the unique properties of CDs composites, such as excellent biocompatibility, outstanding photostability, low toxicity with multicolor emission, they have been widely applied for bioimaging. Among the various applications, majority of reports focus on fluorescence imaging, while a few present other types of imaging (i.e., photoacoustic imaging).

3.1.1. CDs Composites for Fluorescence Imaging

Fluorescence is the most effective tool for tracking the cellular system *in vitro* and *in vivo*, thus fluorescence imaging is one of the most common applications of CDs and their composites in recent years. In general, fluorescence imaging requires a certain ability of photon scattering and light absorption from the imaging probe. As a type of

luminescent materials, CDs have unique PL properties and high QYs, which makes them suitable as probes for fluorescence imaging²²⁹⁻²³¹. Despite the advantages, CDs also face challenges, for example, it's generally difficult to access red/NIR emitting CDs and functional CDs with tissue- or cellular compartment- specificity²³². In this context, heteroatom (i.e., N, S, P) doping and surface modifications are among the most effective means to improve the fluorescence properties of CDs, and thus are commonly applied for all kinds of bioimaging²³³⁻²³⁵.

For most *in vitro* cell imaging, CDs composites were generally found to accumulate in cell membranes and cytoplasm (**Figure 8A**)²³⁶⁻²³⁸, only a few examples demonstrated the ability of entering and imaging the nucleus^{239, 240}. To enhance the imaging specificity of CDs, it is a common practice to conjugate additional targeting moieties. For instance, Wu and co-workers reported PEI-ML-CDs, which could specifically target and image lysosome due to the presence of morpholine group²⁴¹. Lu et al. reported dopamine-CDs composites which could penetrate cell membrane and distribute in the cytoplasm region in AGS and K562 cells²⁰². In addition, Zhang et al. synthesized CDs-AIE through supramolecular assembling of CDs and hydrophobic AIEgen. The CDs-AIE exhibited superior imaging ability *in vivo* and could be ideal fluorescent probe for noninvasive long-term tracing and imaging applications¹⁸⁵.

Multiplex fluorescence imaging exhibits the advantage of detecting multiple emissions from a single fluorescent source, and thus the images have higher resolution²⁴². Recently, applications of CDs composites in multiplex fluorescence imaging have been reported²⁴³⁻²⁴⁶. Zhang and co-workers synthesized Au-CDs and successfully applied this system for the ratiometric fluorescence imaging to monitor Fe³⁺ level in cells, in which both blue and red channels were excited under a single excitation (**Figure 8B**)²⁴⁷. Fe³⁺ can significantly quench red fluorescence through combining with the COOH and NH₂ groups on the surface of Au-CDs; however, the change of blue fluorescence is very small. With the addition of 30 μM Fe³⁺ to osteoblast cells after 10 h, the fluorescence of the red channel was almost quenched,

however, there was almost no change in blue channel. To explore the interactions of M@CDs (M: Ag, Au, Ga, Sn and Zn) with neurons, Vijay et al. co-cultured M@CDs with PC12 cells and the images showed the differentiation progress of the cells at different time intervals, which demonstrated the potential application of M@CDs in neural tissue engineering¹⁰³. Furthermore, by compounding CDs with specific small molecules, CDs composites could exhibit unique properties. For instance, FA can bind to the folate receptors on the surface of cancer cell membranes and then enter cells *via* receptor-mediated endocytosis with non-immunogenicity²⁴⁸. Zhao et al. reported FA@CDs for specific anchoring to the nucleus of MCF-7 cells and the cytoplasm of HepG-2 cells²⁴⁹. The confocal laser scanning microscopy images showed the receptor-mediated endocytosis, expression level of FR, and target recognition of cancer cells of the fluorescent FA-CDs. Furthermore, FA@CDs were further applied for nucleus-targeting photodynamic therapy (PDT) in H413 cells, and the result showed FA@CDs could function as targeting and delivering agents, and thus enhanced PDT efficiency²⁵⁰.

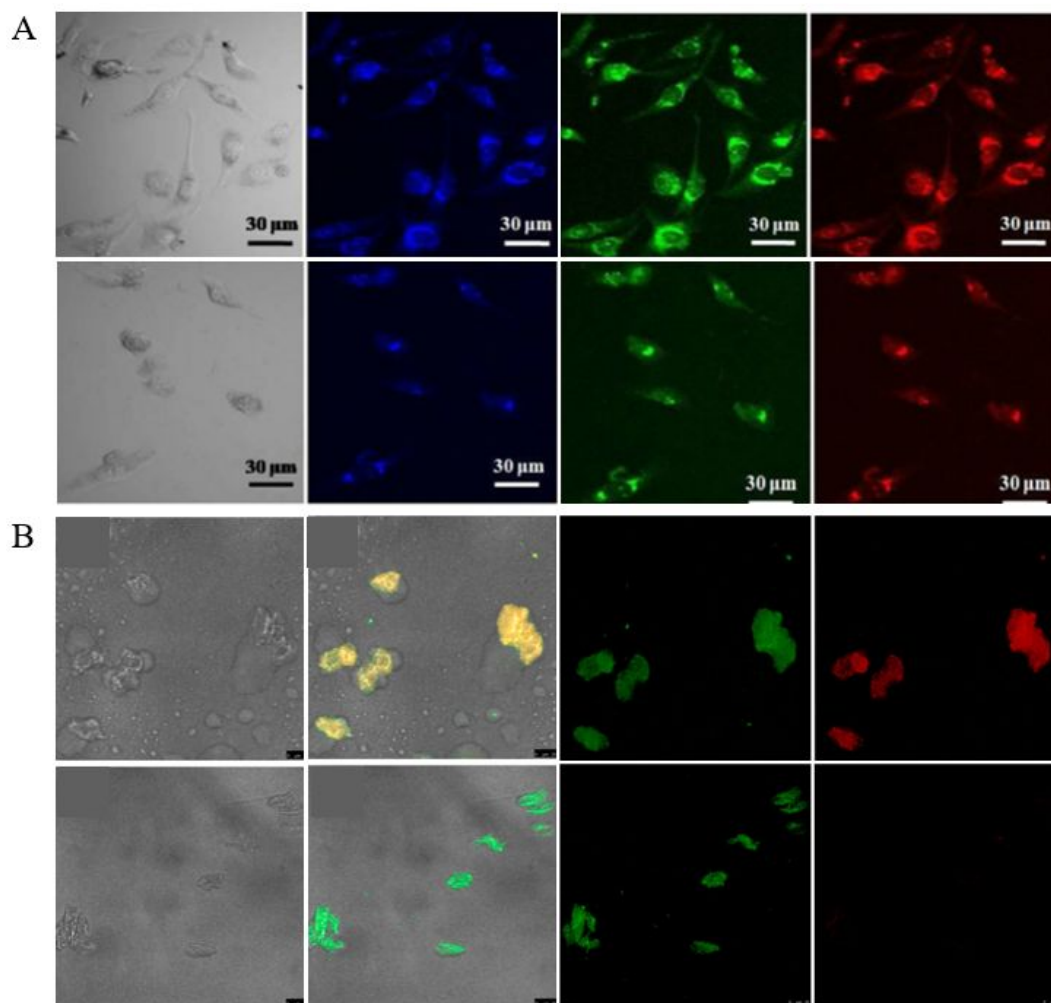


Figure 8. **A)** Laser scanning confocal microscope (LSCM) images of 786–0 cells incubated with 0.30 mg/mL N-CDs/10 mM Fe²⁺(top) and Fe³⁺(bottom). The first, second, third and fourth panels are cell images taken of bright field, 405/422±25, 488/500±25, and 543/650±25 nm ($\lambda_{ex}/\lambda_{em}$), respectively. Reproduced with permission from ref ²³⁶. Copyright 2014, Elsevier. **B)** Fluorescence images of MC3T3-E1 cells incubated with Au-CDs in the absence (top) / presence (bottom) of 30 μ M Fe³⁺. The first, second, third and fourth panels are cell images taken from bright-field, overlay of fluorescence images, blue channel and red channel. Reproduced with permission from ref ²⁴⁷. Copyright 2016, American Chemical Society.

For *in vivo* fluorescence imaging, CDs are expected to emit light with long wavelengths; however, most CDs are often emitted in the blue or green regions²⁵¹. Therefore, it is very meaningful to obtain a yellow or red emitting CDs composites and apply them in *in vivo* fluorescence imaging²⁵²⁻²⁵⁴. For instance, Cui et al. injected red emitting CDs (R-CDs) into mice intravenously and observed red fluorescence scattering throughout their bodies. Considering tumor cells specifically recognize

folic acid, the authors also prepared a folic acid @R-CDs nanomaterial composite. After injecting folic acid @R-CDs into tumor-bearing nude mice for 24 h, the images showed that red fluorescence concentrated at the tumor site and positively correlated with the concentration of the composites (**Figure 9 A-D**)²⁵⁵. In a different study, Lu and co-workers injected dopamine-CDs composites into the back of a mouse and a strong fluorescence signal was observed when excitation and emission wavelengths were 540 and 600 nm, respectively²⁰¹. Among the CDs composites applied for *in vivo* fluorescence imaging, there are also many reports with N-doped CDs²⁵⁶. In addition, PEI and polydopamine (PDA) modified CDs have also been reported and achieved excellent *in vivo* fluorescence imaging (**Figure 9 E-H**)^{257, 258}.

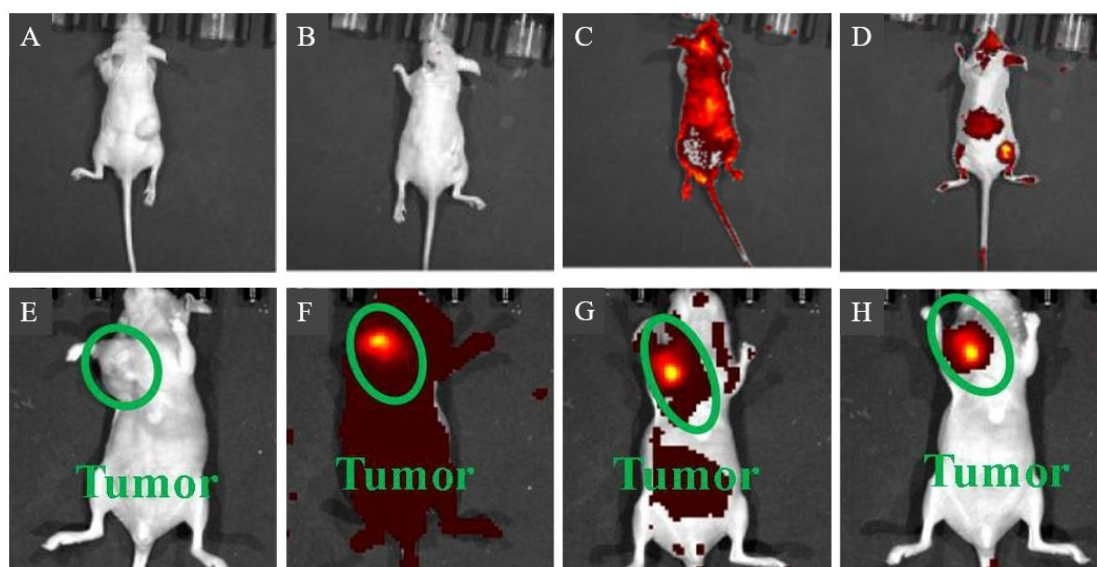


Figure 9. *In vivo* fluorescence images of HepG2 tumor mice after intravenous injection of **A)** saline, **B)** folic acid, **C)** R-CDs, **D)** folic acid@R-CDs. Reproduced with permission from ref ²⁵⁵. Copyright 2019, American Chemical Society. *In vivo* fluorescence images of nude mice after intravenous injection of PDA@N-CDs (Mn) NPs in nude mice for **E)** 0, **F)** 3, **G)** 6, **H)** 12 h. Reproduced with permission from ref ²⁵⁸. Copyright 2019, Elsevier.

3.1.2. CDs Composites for Non-PL Imaging

As discussed above, fluorescence-based imaging techniques for *in vivo* imaging applications are sometimes restricted due to the limited tissue penetration depth and tissue auto fluorescence interference. To bypass these restrictions, photoacoustic (PA) imaging has been developed, making imaging above the optical diffusion limit

feasible through the integration of optical excitation with ultrasonic detection based on the PA effect. Compared to fluorescence imaging, PA imaging could provide deeper tissue-imaging penetration and higher spatial resolution, which is very suitable for real-time and noninvasive diagnosis of diseases²⁵⁹. As such, CDs composites (N-CQDs, GNR@SiO₂-CDs) with high photostability and strong absorption in the near-infrared region (NIR) have been developed and applied for non-invasive PA imaging^{260, 261}. For instance, P, N-CQDs were used as both PA and fluorescence imaging agent for cancer diagnosis²⁶². The P, N-CQDs showed dual wavelength emissions in green and red where QYs were 30% and 78%, respectively. The results revealed that P, N-CQDs were taken up by RAW 264.7 cells and mainly incorporated into the cytoplasm region surrounding the nucleus. The PA images of the tumors showed that P, N-CQDs extravagantly amassed in the tumor and preserved relatively constant PA signals after extended circulation in blood vessels during the whole imaging process (**Figure 10A**). The organs and tissues were removed and imaged (**Figure 10B**), and the results showed tumor and liver tissue exhibited strong fluorescence intensity (**Figure 10C**). Otherwise, the intensities of tumor increased with time after injection, and the green emission reached maxima at near about 3 h post-injection, while the red emission at 6 h (**Figure 10D**).

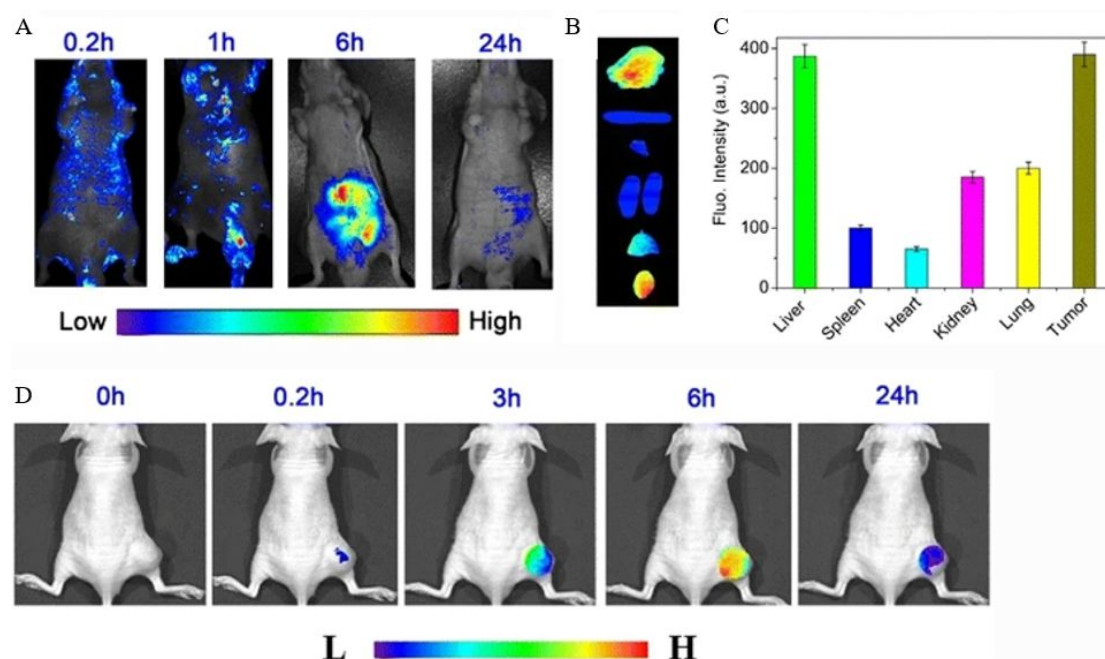


Figure 10. **A)** *In vivo* PA images after intravenous injection of P, N-CQDs in nude mice for different time. **B)** *Ex vivo* images of mice tissues from top to bottom: heart, liver, spleen, lung, kidneys, and tumor. **C)** Fluorescence intensity graph of different mice tissues after intravenous injection of P, N-CQDs. **D)** *In vivo* PA images of nude mice after intravenous injection with P, N-CQDs for different time. Reproduced with permission from ref²⁶². Copyright 2017, Springer Nature.

In addition to PA imaging, magnetic resonance imaging (MRI) is another commonly used imaging technique with excellent sensitivity and high spatial resolution. MRI is regarded as one of the most powerful techniques in modern diagnostic medicine, which has the advantages of high spatial resolution and lacking X-ray radiation, providing anatomical details and high quality three-dimensional images of soft tissue in a non-invasive monitoring manner²⁶³. Due to their excellent magnetic properties and contrast efficiency, Fe^{2+} , Mn^{2+} , and Gd^{2+} are commonly used as MRI contrast agents^{264, 265}. However, the depositions of these metal ions *in vivo* cause biosafety concerns, limiting their practical applications for *in vivo* imaging^{266, 267}. Excitingly, studies showed that doping these ions on CDs could effectively reduce their leakage to a great extent, increase their longitudinal relaxation rate, and show a better magnetic resonance effect²⁶⁸⁻²⁷⁰. For instance, systems based on Gd-CDs and Mn-CDs composites have been developed and applied as MRI probes, respectively^{271, 272}. For the Gd-CDs as MRI probe, it was observed that the Gd-CDs were quickly excreted by kidney and accumulated in bladder after 30 minutes intravenous injection into the mice (**Figure 11A**)²⁷³. In another report, the T1-weighted images of Gd@C-dots-Cys-ZEGFR:₁₉₀₇ in HCC827 tumor xenografts nude mice models showed that SBR/SBR0 at 1 h after injection was higher than that before and 2 h or 4 h after injection (**Figure 11B**)²⁷⁴. Zhao et. al. also reported a Gd/Yb@CDs composite with excellent photostability and MRI signal. Interestingly, this composite could accumulate at tumor area through free tumor vessels with enhanced permeability and retention, making it a potential cancer diagnosis sensor through MRI imaging (**Figure 11C**)²⁷⁵.

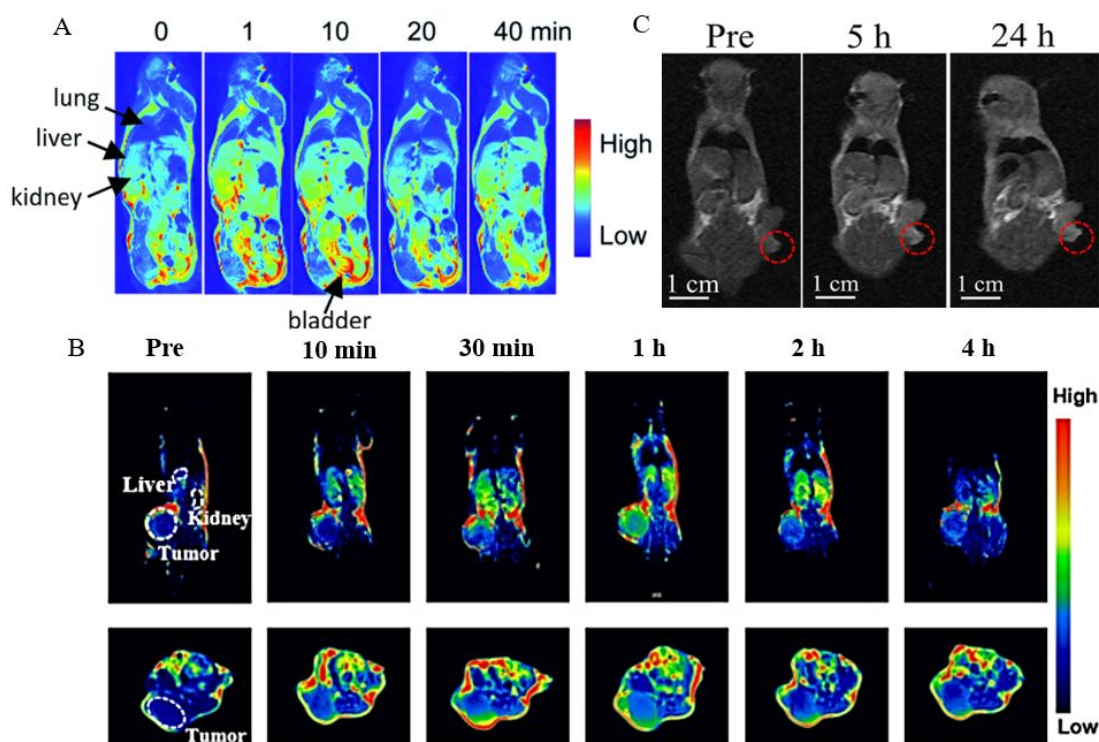


Figure 11. A) *In vivo* T1-weighted MR images of mice after intravenous injection of Gd-CDs for different time. Reproduced with permission from ref ²⁷³. Copyright 2015, Royal Society of Chemistry. B) *In vivo* MR images of HCC827 tumors in mice after intravenous injection of Gd@CDs-Cys-ZEGFR:1907 for different times. Reproduced with permission from ref ²⁷⁴. Copyright 2020, Royal Society of Chemistry. C) *In vivo* MR images of mice after intravenous injection of Gd/Yb@CDs for different time. Reproduced with permission from ref ²⁷⁵. Copyright 2018, American Chemical Society.

CDs are known to have many superior properties, such as excellent PL properties, high biocompatibility as well as economic and easy accessibility. These unique properties render them as excellent candidates for fluorescence imaging agents. However, due to the very nature of CDs (i.e., broad size distributions, non-magnetisms), their applications in bioimaging are generally limited to PL imaging. As discussed above, the applications of CDs in bioimaging could be greatly extended (i.e., PA, MRI imaging) *via* compositing with other materials. Thus, the continuous pursuit of CDs-derived composite materials is of great importance for the further development of CDs-based bioimaging applications.

3.2. CDs Composites for Drug Delivery

Due to their small size, high surface area, excellent fluidity, biocompatibility, easy surface functionalization and intrinsic fluorescence properties, CDs have potential in the application of drug delivery systems (DDS) construction. CDs cannot only transport drugs into cells, but also can be served as a bioimaging agent for tracking drugs. The doping of metal/non-metal ions and surface functionalization could further promote the properties of CDs, increasing the applicability of CDs composites in drug delivery related applications.

3.2.1. CDs Composites for Anti-Cancer Drug Delivery

Doxorubicin (DOX) is a commonly used anticancer drug for tumor cure, it functions by breaking the DNA chain for replication, thus prevents the helix from being resealed and thereby stops the process of tumor replication²⁷⁶. However, due to the nonspecific drug giving, chemotherapy (cure of cancer using chemicals such as DOX) generally faces significant challenges from side effects. As such, various CDs composites have been tested to accurate treatments and avoid drug side effects through designing and constructing structures and functions together with diagnostic, self-targeting, and drug-delivery functions in anticancer treatment^{277, 278}. In DDS constructions, DOX could be attached to CDs or their composites *via* π - π stacking interaction, weakening the fluorescence of CDs through the fluorescence resonance energy transfer (FRET) mechanism²⁷⁹⁻²⁸¹. After delivered to tumor cells, DOX could be released from CDs or their composites upon proper stimulations (i.e., pH change, light excitation, etc.), killing cancer cells specifically and effectively²⁸². This process could also restore the fluorescence of CDs that was previously quenched, the phenomenon of which could be used to track the location of DOX.

Among the various reports, N-CDs were often combined with DOX for anticancer drug delivery (**Figure 12A**)²⁸³. For instance, Gong et al. reported N-CDs as a nanocarrier for cancer therapy, which exhibited high quality single- and two-photon

fluorescence (QY=45%), realizing the real-time monitoring of the endocytosis, intracellular distribution and release of DOX (**Figure 12B**)²⁸⁴. In addition, metal and organics-CDs composites were also used to combine with DOX as DDS²⁸⁵⁻²⁹⁰. For instance, Yao et al. prepared magneto fluorescent CQDs (MFCQDs) using a combination of waste crab shell and three different transition-metal ions (Gd^{3+} , Mn^{2+} , and Eu^{3+}) by microwave-assisted pyrolysis. These composites could integrate with DOX and specifically target cancer cells *via* the overexpressed folate receptors²⁹¹. Other groups have synthesized CDs conjugated HAp nanocomposites and applied them simultaneously for PL imaging and DOX delivery (**Figure 12C**)²⁹². In these nanocomposites, CDs were synthesized through the *in situ* mineralization and carbonization of HAp. It's worth noting that DOX molecules were loaded through electrostatic interactions with carboxyl groups and eventually released through a diffusion-controlled mechanism (**Figure 12D**)²⁹³.

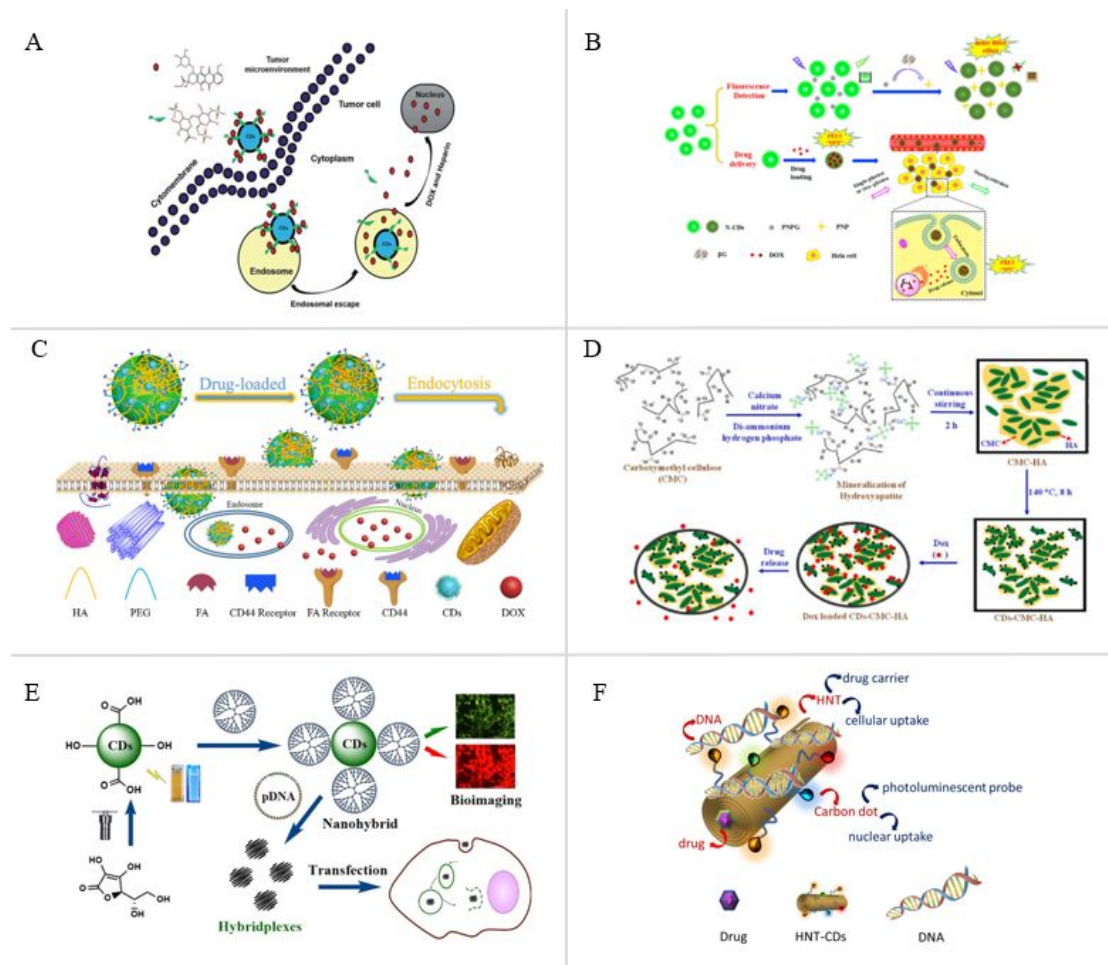


Figure 12. **A)** Illustration of the intracellular release behavior of DOX from the CDs–Heparin/DOX drug delivery system. Reproduced with permission from ref ²⁸³. Copyright 2017, Royal Society of Chemistry. **B)** Illustration of the intracellular release behavior of DOX from the N-CDs/DOX drug delivery system by two-photon fluorescence imaging. Reproduced with permission from ref ²⁸⁴. Copyright 2018, Elsevier. **C)** Illustration of the intracellular release behavior from the DOX-loaded FA-PEG-HAp-CDs theranostic nanogels. Reproduced with permission from ref ²⁹². Copyright 2016, Elsevier. **D)** Schematic illustration of the intracellular release behavior of DOX from CDs decorated carboxymethyl cellulose-HAp nanocomposite (CDs-CMC-HAp). Reproduced with permission from ref ²⁹³. Copyright 2017, Elsevier. **E)** Representation of the preparation of CDs@PAMAM nanohybrids and the applications for bioimaging and gene delivery. Reproduced with permission from ref ¹⁹⁹. Copyright 2021, American Chemical Society. **F)** Cartoon representation of HNT-CDs multifunctional nanocarrier. Reproduced with permission from ref ²⁹⁴. Copyright 2019, Elsevier.

Paclitaxel (PTX) is another commonly used anticancer agent, which can affect nuclear morphology and promote apoptosis through interacting with microtubule polymer and restraining dissociation of tubulin^{295, 296}. Jennifer et al. synthesized N-CDs by microwave-assisted method and constructed a DDS by coupling these CDs with PTX *via* a carbodiimide condensation reaction. In this DDS, PTX could be readily released from N-CDs carriers after internalization due to the hydrolysis of the ester bond between PTX and N-CDs^{297, 298}. Unfortunately, unlike in other reports, the anticancer efficiency of the PTX conjugates was not better than that of free PTX, they held similar efficiencies. Metronidazole (MET), as an antibiotic, can cause strand damage to the bacterial DNA through the reduction of its nitro-group by an electron transport protein²⁹⁹. Sara et al. reported conjugated cCQD-MET could rapidly internalize into the H413 cells and exhibit enhanced antimicrobial activity³⁰⁰. In a different study, the CDs@PtPor composite demonstrated strong photocytotoxicity under light irradiation and therapeutic efficacy as well as low side effects *in vitro*, which was developed as drug nanocarrier in the cancer therapy¹⁸⁴.

3.2.2. CDs Composites for Gene Delivery

In addition to antitumor drug delivery, there have also been significant interests on the applications of CDs composites for gene delivery^{301, 302}. Gene delivery is the process of introducing foreign DNA into host cells³⁰³, and could be regarded as a special case of “drug” delivery. Gene delivery is one of the necessary steps required for gene

therapy and genetic modifications³⁰⁴. Gene delivery systems could protect genetic materials from premature degradation during the systemic blood circulation and effectively transport therapeutic genes to the target cells³⁰⁵. CDs are extremely suitable for gene transmission due to their rich surface functionalities. Firstly, the rich presence of surface functionalities endows CDs with excellent water solubility; Secondly, one can engineer the surface functional groups of CDs so that the loading and release of gene therapeutics could be precisely controlled through the interactions (i.e., covalent interaction) of the two³⁰⁶⁻³⁰⁸. Among the various CDs composites, PEI-CDs composites have been paid much attention due to their synthetic maneuverability and high DNA-binding ability³⁰⁹⁻³¹¹. For instance, both Dou and Liu's groups have reported PEI functionalized CDs applied for DNA delivery^{204, 312}. It's worth to mention that in these systems, PEI molecule played two roles: 1) as the surface passivation agent to enhance the fluorescence of CDs; 2) as polyelectrolyte to condense DNA through electrostatic interactions. Further, PEI-CDs have also been composited with folic acid/hyaluronic acid /fluorine/nitrogen and applied for gene delivery³¹³⁻³¹⁶. In addition, Ivo et al. reported (polyamidoamine)-PAMAM-NH₂-CDs nanohybrids for DNA delivery. The nanohybrids showed mild cytotoxicity and presented very high transfection efficiencies(**Figure 12E**)¹⁹⁹. Marina and co-workers established a CDs@HNT-DNA model through electrostatic interactions between CDs@HNT with DNA. And the result showed that the model did not cause alteration in the DNA structure and DNA was slowly released through a dialysis membrane in physiological media(**Figure 12F**)²⁹⁴.

3.3. CDs Composites for Optical Biosensing

Biosensors, including enzymatic sensors, immunosensors, and nucleic acid sensors, are analytical devices used to detect important organic or inorganic molecules in organisms, which combine biological components with physicochemical detectors^{317, 318}. Recently, applications of CDs and their composites in biosensing have been widely investigated³¹⁹. Thanks to the unique properties of CDs, sensors derived from CDs and their composites demonstrate various advantages: 1) tunable PL emissions,

which render the sensors with superior optical sensing abilities; 2) excellent PL stability, which could avoid many analysis errors caused by the degradation of fluorescent probes; 3) extremely low toxicity of the sensors due to the very nature of CDs (i.e., carbon composed), which warrants their eventual *in vivo* applications; 4) rich presence of surface functionalities in the CDs composites, which can provide abundant binding sites for specific bioreceptors that is an essential part in biosensing process; 5) most importantly, by composition with other materials, sensors derived from CDs could demonstrate high sensitivity and selectivity towards some specific detection objects (i.e., enzymes, nucleic acids)³²⁰⁻³²². Therefore, studies focusing on the combining of CDs with various materials for the development of CDs composites-derived sensing systems have been widely reported.

Optical sensors are among the most investigated CDs composites-derived systems. In such a typical optical biosensor, specific targets could be bound to CDs composites and being recognized by bioreceptors. During this process, interactions of target analytes and CDs composites could interfere the optical signals of CDs composites; by monitoring the alternation of the optical signals, information (i.e., concentrations) regarding the target analytes could be obtained. Generally speaking, based on their sensing mechanisms, the sensors could be divided as three classes, namely “on-off”, “on-off-on” and “off-on-off” (**Figure 13**).

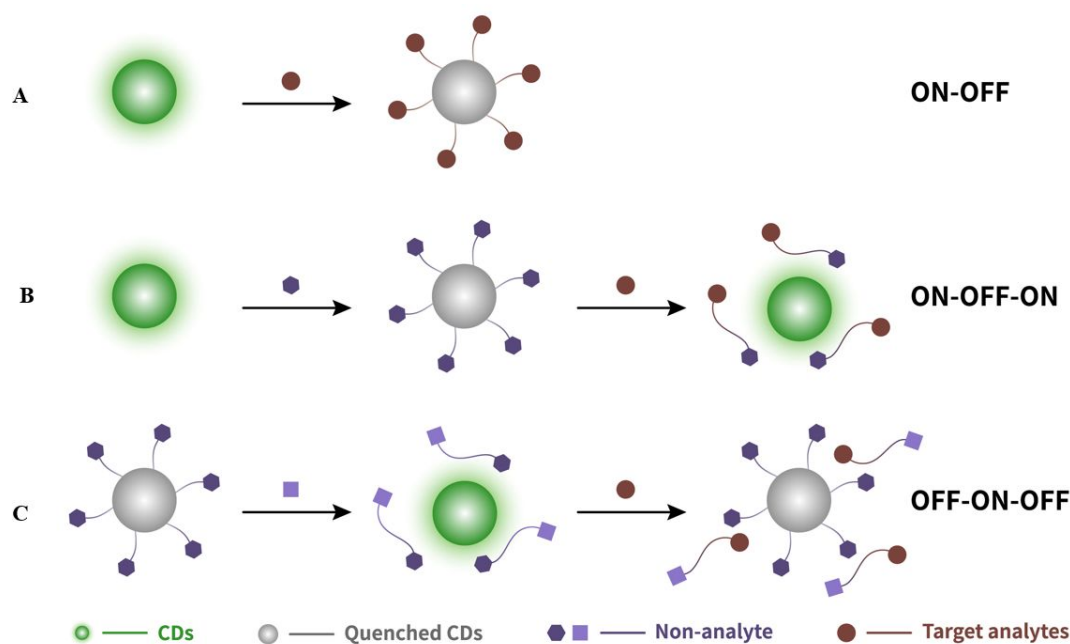


Figure 13. Cartoon representations of typical optical biosensing strategies: **A)** “on-off” strategy; **B)** “on-off-on” strategy; **C)** “off-on-off” strategy.

The type of “on-off” sensors relies on the decrease (or even complete quenching) of CDs composites PL to detect the target analytes. In other words, by developing a negative correlation between the PL intensity of CDs composites and the concentration of the target analyte, the concentration of an unknown sample could be calculated from the calibration curve developed (**Figure 13A**). Currently, various mechanisms have been elucidated. Among them, three main mechanisms for PL quenching, namely forster resonance energy transfer (FRET)³²³⁻³²⁵, photoinduced electron transfer (PET)³²⁶⁻³²⁸ and inner filtering effect (IFE)³²⁹⁻³³¹ have been widely used for the design and development of CDs composites-based optical biosensors. On the other hand, in a typical “on-off-on” biosensor, the optical signal of CDs composites undergo a stepwise change: the PL is first turned off due to the interaction with a non-analyte quencher, then it could be restored in the presence of the target analyte; thus the degree of recovery of the PL of the CDs composites could be used for the detection and determination of the target analyte (**Figure 13B**)^{332, 333}. Although uncommon, sensing platform based on “off-on-off” strategy has also been reported³³⁴, in which the quenched PL could be restored due to the interaction with a non-analyte, then the PL could be turned off again in the presence of the target analyte (**Figure**

13C). With these sensing strategies, CDs composites-derived sensors have been widely developed and achieved great success in the detection and determination of substances such as biologically important molecules³³⁵⁻³³⁷, environmentally concerned substances³³⁸ as well as metal ions³³⁹⁻³⁴¹.

3.3.1. CDs Composites for the Sensing of Biologically Important Molecules

There are many biologically important molecules closely related to our health, their presence in proper concentrations are essential for body functions. Thus, it is important to develop facile and reliable sensors to monitor these molecules^{342, 343}. Glutathione (GSH) and cysteine (Cys) are such molecules that could prevent reactive oxygen species from destroying cellular components. Following the “on-off” strategy, Wu et al. established a fluorometric nanoprobe with N-doped CDs for the sensitive detection of GSH, in which the PL of CDs was in reverse relationship with the concentration of GSH due to the thiol group triggered IFE^{344, 345}. On the other hand, Cai and co-workers designed novel “on-off-on” biosensors using CDs–MnO₂ nanocomposites for the sensing of GSH^{346, 347}. In this system, PL of CDs was initially quenched by the MnO₂ nanosheets through energy transfer between the two; in the presence of the target analyte GSH, the MnO₂ nanosheets were reduced to Mn²⁺ ions, causing the release of CDs and restoration of CDs PL (**Figure 14A**).

Alkaline phosphatase (ALP) in serum is another biologically important molecule, which is closely related to various diseases including cancer and bone disease; therefore, the sensitive detection of ALP is also of great importance³⁴⁸. As such, Li et al. established a sensing platform with N-doped CDs (QY=49%) for the quick and sensitive detection of ALP. In this system, CDs were presented together with *p*-Nitrophenylphosphate (PNPP), a substance that could be transformed into *p*-nitrophenol (PNP) under the catalysis of ALP. Since the emission of CDs and the absorption of PNP overlap very well, PL of CDs could be effectively quenched through IFE by PNP, thus realizing the sensing of ALP³⁴⁹.

In addition to molecules discussed above, nucleic acids are another class of biologically important molecules, as a result, sensing platforms designed for the detection of nucleic acid based on CDs composites have also been heavily studied^{350, 351}. For instance, Somaye et al. developed an ultrasensitive homogeneous biosensor for the detection of HIV-related DNA sequences, the sensing of which was realized by FRET between CDs and AuNPs^{352, 353}. Interestingly, the PET mechanism was also adopted to detect DNA using CdTe–CDs as probe and Mitoxantrone as an “on-off-on” signal reagent³⁵⁴. In addition to the above examples, the sensing of other biologically important molecules such as ATP, trypsin, dopamine, glucose and RNA have also been successfully realized using CDs composites as probes³⁵⁵⁻³⁶³.

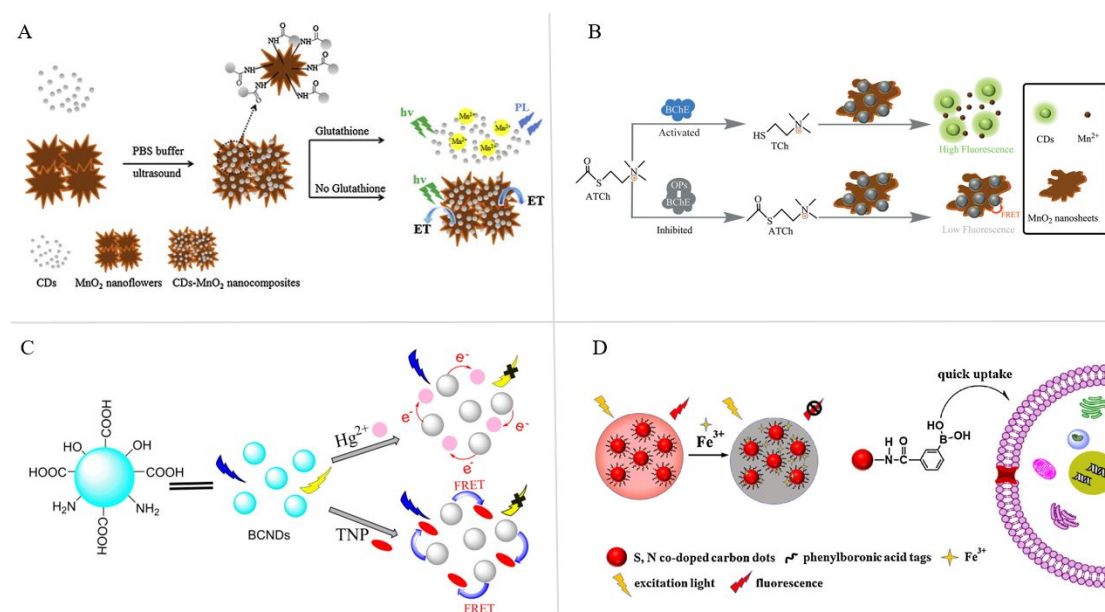


Figure 14. **A)** Schematic illustration of CDs–MnO₂ nanocomposites for GSH detection. Reproduced with permission from ref ³⁴⁷. Copyright 2015, Elsevier. **B)** Schematic illustration of CDs–MnO₂ nanosheets for OPs detection (“off-on-off” strategy). Reproduced with permission from ref ³³⁴. Copyright 2018, American Chemical Society. **C)** Schematic illustration of N, B-doped CDs for sensing Hg²⁺ and TNP. Reproduced with permission from ref ³⁶⁴. Copyright 2016, Elsevier. **D)** Schematic illustration of N, S-CDs-PBA for sensing Fe³⁺ in PC12 cells. Reproduced with permission from ref ³⁶⁵. Copyright 2018, Elsevier.

3.3.2. CDs Composites for the Sensing of Environmentally Concerned Substances

Organophosphorus compounds (OPs) are the most widely used pesticide in modern agriculture. Due to their strong inhibitory effects on cholinesterase, they have great threat to human health. Therefore, attempts to detect OPs with CDs composites-based sensors have been frequently carried out³⁶⁶⁻³⁶⁹. For instance, Hou et al. developed a system based on quarternized CDs (Q-CDs) for the detection of dichlorvos. In this sensing system, the detection of the analyte was realized through a FRET process, in which 5-thio-2-nitrobenzoic acid anion (TNB) acted as the energy acceptor while Q-CDs as the energy donors. The sensor was based on Ellman's test: acetylcholinesterase (AChE) can catalyze the forming of TNB, which can quench the fluorescence of Q-CDs, and dichlorvos can inhibit the activity of AChE, which can recover the fluorescence of Q-CDs, forming the "on-off-on" sensor³⁷⁰. Following the same mechanism, Yan et al. developed an "off-on-off" fluorescence platform for the sensitive detection of OPs by utilizing MnO₂-CDs nanosensor³³⁴ (**Figure 14B**). Specifically, the quenched PL of CDs by MnO₂ nanosheets through FRET was first recovered by adding butyrylcholinesterase (BChE) and acetylthiocholine (ATCh). However, the BChE activity could be significantly inhibited in the presence of OPs, causing the PL of CDs was quenched again, and thus realizing the detection of OPs. It's worth to mention that MnO₂ nanosheets served not only as the nanoquencher but also recognition unit for OPs in this sensing platform.

Known as picric acid, 2,4,6-Trinitrophenol (TNP) is a general precursor for the production of fireworks, explosives and dyes with low safety factor and strong explosive ability³⁷¹. Thus, the accurate and sensitive detection of TNP is also very important^{372, 373}. To detect TNP, Ye et al. developed a TNP sensing platform using N, B-doped CDs. This system demonstrated a high sensitivity towards TNP, the limit of detection was 0.35 μM (**Figure 14C**)³⁶⁴. Exploiting similar sensing mechanism, Wang et al. also developed a platform using mesoporous SBA-15 functionalized with

3-glycidyloxypropyltrimethoxysilane and multi-hydroxyl CDs as probe with the limit of detection down to $0.17 \mu\text{M}$ ³⁷⁴. Interestingly, (3-chloro-2-hydroxypropyl) trimethylammonium chloride functionalized CDs synthesized by Gao et al. had much lower detection limit down to 70.4 nM ³⁷⁵. In addition to the above-mentioned substances, other environmentally concerned molecules such as drugs, tetracycline, H_2O_2 , and H^+ (pH) have also been successfully detected and determined by CDs composites-based sensing platforms³⁷⁶⁻³⁸².

3.3.3. CDs Composites for the Sensing of Metal Ions

Metal ions play important roles in various physiological activities and are essential chemicals for all lives. Therefore, sensing methods for the highly sensitive and selective detection of metal ions in biological systems are greatly desired. As such, there have been many studies focusing on the applications of CDs composites as fluorescent probes for metal ion detection^{383, 384}. Generally speaking, most of the sensing platforms for the detection of metal ions were designed by following the “on-off” strategy^{385, 386}. When interact with CDs composites, the empty *d* or *f* orbitals of the metal ions could host the energized electrons from the excited states of CDs, and thus effectively quench the PL of CDs through PET. As a result, most of the sensing platforms were designed by utilizing the PET between CDs composites and metal ions. For instance, Li et al. reported a N and S co-doped CDs (N, S-CDs)-based sensor for the sensitive detection of Hg^{2+} in living cells, the sensing of which was achieved through the PL quenching of N, S-CDs caused by the electron-transfer and coordination interaction between N, S-CDs and Hg^{2+} ion³⁸⁷. Following the same strategy, another group successfully accomplished the sensing of Fe^{3+} ions using a system in which N and S co-doped CDs were tagged with phenylboronic acid (N, S-CDs-PBA)³⁶⁵. In this specific system, Fe^{3+} could coordinate with phenolic hydroxyl and carboxyl groups on the surface of CDs and thus excited electrons of N, S-CDs-PBA were transferred to Fe^{3+} , causing the PL quenching (**Figure 14D**). Although as not frequent as PET, FRET was also a common mechanism used for

detection of metal ions. For instance, in Yan and co-workers' study, glyoxylic acid-modified CDs (GA-CDs) were used as a FRET ratiometric fluorescent probe for the detection of Cu^{2+} in aqueous solution³⁸⁸. Similarly, Chen et al. also applied cyclam-functionalized CDs as FRET nanoprobe for the detection of Cu^{2+} and S^{2-} ³⁸⁹. In addition to the above examples, the detection of other important metal ions such as Ag^+ , Cu^{2+} , Cr^{6+} , Pb^{2+} have also been successfully realized with CDs composites-based sensing platforms³⁹⁰⁻⁴⁰¹.

4. Summary and Outlook

In this review, recent advancements of CDs-derived composites from their synthetic routes to bioapplications have been comprehensively summarized. First, we briefly introduced the properties, synthesis methods and applications of CDs. Then we carefully discussed the synthesis approaches for four types of CDs composites, namely metal-CDs, nonmetallic inorganics-CDs, organics-CDs and multi-components-CDs composites. After that, the recent advancements of these CDs composites for their applications in the biomedical fields were also detailed. As discussed, CDs composites have unique fluorescence and biological properties, rendering them as suitable platforms for biomedical research, which was witnessed by the ever-increasing reports on this topic. Despite the above-mentioned advancements, studies on the preparation, characterization and applications of CDs composites are still in their early stage, and there are several challenges that need to be addressed.

Current synthesis of CDs composites generally requires two or more steps to complete, which not only demands high manufacturing costs, but also causes significant complexities in their characterizations and applications. Also, the construction of CDs composites is highly empirical and heavily relies on a "trial and error" approach! Thus, there is an urgency to streamline the current synthesis approaches for CDs composites, so that rational design of CDs composites could be realized. Furthermore, most of CDs composites have not been properly isolated and purified, leaving them as

mixtures of complex components with very distinct spectroscopic and biological properties after fine fractionalization. Thus, it would make sense to develop convenient and effective separation techniques to purify the as-prepared CDs composites so that samples with better uniformity could be obtained. To fulfill the potential industrial applications of CDs composites, in addition to the streamlined synthesis and utilization of convenient but effective purification techniques, researchers should also focus on the development of low cost and large-scale production of CDs. Although there have been a few groups reported the large-scale (i.e., kilogram-scale) preparation of CDs^{231, 402}, currently, the preparation of CDs in large-scale is still very hard to achieve. Recently, Xiong's group reported a novel strategy for the large-scale preparation of NIR CDs with solid-state reaction, in which neither high pressure reactors nor complicated post-treatment procedures were required⁴⁰³. This safe, convenient synthesis approach might provide some inspiration for the mass production of CDs and CDs composites that meet for the industrial requirements.

Much effort has been devoted for the syntheses and bioapplications of CDs and CDs composites; however, their biocompatibility and nano safety issues have been less concerned. Generally speaking, carbon-based materials are inherently less toxic than metal- or semiconductor-based materials considering the intrinsic nature of carbon. Still, the cytotoxicities of CDs have raised much concern⁴⁰⁴⁻⁴⁰⁶, since the toxicity of bare CDs are often dose and time dependent⁴⁰⁷. Surprisingly, there has been report that CDs derived from the same precursors, but with different synthesis methods demonstrated different cytotoxicities⁴⁰⁸. As such, researchers should devote more efforts to study and evaluate the bio-related properties of bare CDs. As regarding to the biosafety of CDs composites, things become more complicated since additional

components (i.e., metals, nonmetallic inorganics and organic molecules) are introduced, thus these factors should be carefully reevaluated. For instance, doping with metals has been a conventional strategy to enhance the PL of CDs, however, this might reduce the biocompatibility of CDs, since some of the metals might increase the toxicity of CDs composites significantly. On the other hand, compositing with some materials (i.e., polymers) indeed improves the biological properties of CDs, however, the enhancement of the PL performance may not be as good as by doping with metals. Thus, to obtain CDs composites with superior properties for bioapplications, the types and ratios of compositing materials have to be carefully balanced! And a proper evaluation method of the cytotoxicity and biocompatibility of CDs composites should be carefully selected, so that biosafety of CDs composites in the context of bioapplications could be accurately and adequately assessed.

Still, we anticipate much more efforts will be devoted to CDs composites and much more exciting CDs composites-based applications in the biomedical fields will be developed. Especially with the streamline of the synthesis methods, introduction of effective purification techniques and accurate and adequate biosafety evaluations, CDs composites with controlled compositions, tailored properties, and high biocompatibility would be feasible, which would significantly accelerate the applications of CDs composites in biomedicine related fields.

Acknowledgements

Z. Peng gratefully acknowledge the financial support from the National Natural Science Foundation of China under the grant number: 21807010, and the Applied Basic Research Program of Yunnan Province under the grant number: 2019FB066. R. M. Leblanc gratefully acknowledges the support of the National Science Foundation under Grants 1809060 and 2041413.

Declaration of Interests

The authors declare that they have no known competing financial interests or personal relationships that could have appeared to influence the work reported in this paper.

References

1. S. Gogoi, S. Maji, D. Mishra, K. S. P. Devi, T. K. Maiti and N. Karak, *Macromol Biosci*, 2017, **17**, 1600271.
2. X. Xu and R. Ray, *J. Am. Chem. Soc.*, 2004, **126**, 12736.
3. Y.-P. Sun, B. Zhou, Y. Lin, W. Wang, K. S. Fernando, P. Pathak, M. J. Meziani, B. A. Harruff, X. Wang and H. Wang, *J. Am. Chem. Soc.*, 2006, **128**, 7756-7757.
4. S. Ganguly, P. Das, S. Banerjee and N. C. Das, *Funct. Compos. Struct.*, 2019, **1**, 022001.
5. L. Ai, Y. Yang, B. Wang, J. Chang, Z. Tang, B. Yang and S. Lu, *Science Bulletin*, 2021, **66**, 839-856.
6. J. Yu, X. Yong, Z. Tang, B. Yang and S. Lu, *J. Phys. Chem. Lett.*, 2021, **12**, 7671-7687.
7. A. Cayuela, M. Soriano, C. Carrillo-Carrión and M. Valcárcel, *Chem. Commun.*, 2016, **52**, 1311-1326.
8. Q. Zeng, T. Feng, S. Tao, S. Zhu and B. Yang, *Light: Sci. Appl.*, 2021, **10**, 142.
9. S. Li, L. Li, H. Tu, H. Zhang, D. S. Silvester, C. E. Banks, G. Zou, H. Hou and X. Ji, *Mater. Today*, 2021, DOI: <https://doi.org/10.1016/j.mattod.2021.07.028>.
10. S.-L. Hu, K.-Y. Niu, J. Sun, J. Yang, N.-Q. Zhao and X.-W. Du, *J. Mater. Chem.*, 2009, **19**, 484-488.
11. Y.-P. Sun, X. Wang, F. Lu, L. Cao, M. J. Meziani, P. G. Luo, L. Gu and L. M. Veca, *J. Phys. Chem. C*, 2008, **112**, 18295-18298.
12. J. Zhou, C. Booker, R. Li, X. Zhou, T.-K. Sham, X. Sun and Z. Ding, *J. Am. Chem. Soc.*, 2007, **129**, 744-745.
13. L. Tian, D. Ghosh, W. Chen, S. Pradhan, X. Chang and S. Chen, *Chem. Mater.*, 2009, **21**, 2803-2809.
14. D. Pan, J. Zhang, Z. Li and M. Wu, *Adv. Mater.*, 2010, **22**, 734-738.
15. Y. Wang and A. Hu, *J. Mater. Chem. C*, 2014, **2**, 6921-6939.
16. H. Li, F.-Q. Shao, H. Huang, J.-J. Feng and A.-J. Wang, *Sens. Actuators B Chem.*, 2016, **226**, 506-511.
17. L. Pan, S. Sun, A. Zhang, K. Jiang, L. Zhang, C. Dong, Q. Huang, A. Wu and H. Lin, *Adv. Mater.*, 2015, **27**, 7782-7787.
18. S. Miao, K. Liang, J. Zhu, B. Yang, D. Zhao and B. Kong, *Nano Today*, 2020, **33**, 100879.
19. Y. Ru, L. Ai, T. Jia, X. Liu, S. Lu, Z. Tang and B. Yang, *Nano Today*, 2020, **34**, 100953.
20. H. Wang, W. Su and M. Tan, *The Innovation*, 2020, **1**, 100009.
21. Q. Xu, T. Kuang, Y. Liu, L. Cai, X. Peng, T. S. Sreeprasad, P. Zhao, Z. Yu and N. Li, *J. Mat. Chem. B*, 2016, **4**, 7204-7219.
22. Y. Park, J. Yoo, B. Lim, W. Kwon and S.-W. Rhee, *J. Mater. Chem. A*, 2016, **4**, 11582-11603.

23. W. Liu, C. Li, Y. Ren, X. Sun, W. Pan, Y. Li, J. Wang and W. Wang, *J. Mat. Chem. B*, 2016, **4**, 5772-5788.
24. K. Dimos, *Curr. Org. Chem.*, 2016, **20**, 682-695.
25. F. Yan, Z. Sun, H. Zhang, X. Sun, Y. Jiang and Z. Bai, *Microchim. Acta*, 2019, **186**, 583.
26. P. G. Luo, S. Sahu, S.-T. Yang, S. K. Sonkar, J. Wang, H. Wang, G. E. LeCroy, L. Cao and Y.-P. Sun, *J. Mat. Chem. B*, 2013, **1**, 2116-2127.
27. W. Wang, L. Cheng and W. Liu, *Sci. China: Chem.*, 2014, **57**, 522-539.
28. J. Pardo, Z. Peng and R. M. Leblanc, *Molecules*, 2018, **23**, 378.
29. X. Cui, L. Zhu, J. Wu, Y. Hou, P. Wang, Z. Wang and M. Yang, *Biosens. Bioelectron.*, 2015, **63**, 506-512.
30. F. Wang, S. Pang, L. Wang, Q. Li, M. Kreiter and C.-y. Liu, *Chem. Mater.*, 2010, **22**, 4528-4530.
31. S. Anwar, H. Ding, M. Xu, X. Hu, Z. Li, J. Wang, L. Liu, L. Jiang, D. Wang, C. Dong, M. Yan, Q. Wang and H. Bi, *ACS Appl. Bio Mater.*, 2019, **2**, 2317-2338.
32. F. Yuan, S. Li, Z. Fan, X. Meng, L. Fan and S. Yang, *Nano Today*, 2016, **11**, 565-586.
33. K. Nekoueian, M. Amiri, M. Sillanpää, F. Marken, R. Boukherroub and S. Szunerits, *Chem. Soc. Rev.*, 2019, **48**, 4281-4316.
34. J. Pardo, Z. Peng and R. M. Leblanc, *Molecules*, 2018, **23**.
35. H. Wu, W. Su, H. Xu, Y. Zhang, Y. Li, X. Li and L. Fan, *VIEW*, 2021, **2**, 20200061.
36. K. K. Chan, S. H. K. Yap and K.-T. Yong, *Nano-Micro Lett.*, 2018, **10**, 72.
37. H. Ding, X.-X. Zhou, J.-S. Wei, X.-B. Li, B.-T. Qin, X.-B. Chen and H.-M. Xiong, *Carbon*, 2020, **167**, 322-344.
38. D. Li, E. V. Ushakova, A. L. Rogach and S. Qu, *Small*, 2021, **n/a**, 2102325.
39. C. Ji, Y. Zhou, R. M. Leblanc and Z. Peng, *ACS Sens.*, 2020, **5**, 2724-2741.
40. D. Xu, Q. Lin and H.-T. Chang, *Small Methods*, 2020, **4**, 1900387.
41. B. Li, S. Zhao, L. Huang, Q. Wang, J. Xiao and M. Lan, *Chem. Eng. J.*, 2021, **408**, 127245.
42. B. Wang, H. Song, X. Qu, J. Chang, B. Yang and S. Lu, *Coord. Chem. Rev.*, 2021, **442**, 214010.
43. Z. Peng, X. Han, S. Li, A. O. Al-Youbi, A. S. Bashammakh, M. S. El-Shahawi and R. M. Leblanc, *Coord. Chem. Rev.*, 2017, **343**, 256-277.
44. Z. Peng, T. Zhao, Y. Zhou, S. Li, J. Li and R. M. Leblanc, *Adv. Healthc. Mater.*, 2020, **9**, 1901495.
45. F. Zu, F. Yan, Z. Bai, J. Xu, Y. Wang, Y. Huang and X. Zhou, *Microchim. Acta*, 2017, **184**, 1899-1914.
46. F. Li, D. Yang and H. Xu, *Chem. Eur. J.*, 2019, **25**, 1165-1176.
47. Z. Suo, J. Dai, S. Gao and H. Gao, *Results Phys.*, 2020, 103058.
48. L. Ai, R. Shi, J. Yang, K. Zhang, T. Zhang and S. Lu, *Small*, 2021, **n/a**, 2007523.
49. X.-Y. Du, C.-F. Wang, G. Wu and S. Chen, *Angew. Chem. Int. Ed.*, 2021, **60**, 8585-8595.
50. L. Lin, Y. Luo, P. Tsai, J. Wang and X. Chen, *TrAC, Trends Anal. Chem.*, 2018, **103**, 87-101.
51. Y. Zhou, S. K. Sharma, Z. Peng and R. M. Leblanc, *Polymers*, 2017, **9**, 67.
52. N. Tejwan, A. K. Saini, A. Sharma, T. A. Singh, N. Kumar and J. Das, *J. Control. Release*, 2021, **330**, 132-150.
53. A. Beiraghi and S. A. Najibi-Gehraz, *Sens. Actuators B Chem.*, 2017, **253**, 342-351.
54. X. Zeng, Z. Wang, N. Meng, D. T. McCarthy, A. Deletic, J.-h. Pan and X. Zhang, *Appl. Catal. B-Environ.*, 2017, **202**, 33-41.
55. Y. Yao, D. Niu, C. H. Lee, Y. Li and P. Li, *Macromol. Rapid Commun.*, 2019, **40**, 1800869.
56. T. Feng, X. Ai, G. An, P. Yang and Y. Zhao, *ACS nano*, 2016, **10**, 4410-4420.

57. K. Kannan, D. Radhika, K. K. Sadasivuni, K. R. Reddy and A. V. Raghu, *Adv. Colloid Interface Sci.*, 2020, 102178.
58. J. Liu, J. Jiang, Y. Meng, A. Aihemaiti, Y. Xu, H. Xiang, Y. Gao and X. Chen, *J. Hazard. Mater.*, 2020, **388**, 122026.
59. L. Wang, Y. Li, S. Li, Y. Wang, W. Kong, W. Xue and C. Li, *J. Mater. Sci.: Mater. Electron.*, 2017, **28**, 17570-17577.
60. A. Emam, A. Mostafa, M. Mohamed, A.-S. Gadallah and M. El-Kemary, *J. Lumin.*, 2018, **200**, 287-297.
61. X. Li, Y. Fu, S. Zhao, J. Xiao, M. Lan, B. Wang, K. Zhang, X. Song and L. Zeng, *Chem. Eng. J.*, 2021, DOI: <https://doi.org/10.1016/j.cej.2021.133101>, 133101.
62. L. Wang, P. Liu, Z. Liu, H. Cao, S. Ye, K. Zhao, G. Liang and J.-J. Zhu, *Sens. Actuators B Chem.*, 2021, **327**, 128890.
63. S. Barua, P. K. Raul, R. Gopalakrishnan, B. Das, Vanlalhmuaaka and V. Veer, *ACS Sustain. Chem. Eng.*, 2016, **4**, 2345-2350.
64. L.-M. Shen, Q. Chen, Z.-Y. Sun, X.-W. Chen and J.-H. Wang, *Anal. Chem.*, 2014, **86**, 5002-5008.
65. Y. Zhang, B.-T. Zhang, Y. Teng, J. Zhao, L. Kuang and X. Sun, *Sep. Purif. Technol.*, 2021, **254**, 117617.
66. P.-p. Zhu, Z. Cheng, L.-l. Du, Q. Chen and K.-j. Tan, *Langmuir*, 2018, **34**, 9982-9989.
67. J. Cheng, C.-F. Wang, Y. Zhang, S. Yang and S. Chen, *RSC Adv.*, 2016, **6**, 37189-37194.
68. R. Bayan and N. Karak, *ACS Omega*, 2017, **2**, 8868-8876.
69. J. Hua, Z. Mu, P. Hua, M. Wang and K. Qin, *Talanta*, 2020, **219**, 121279.
70. J. M. Arroyave, M. E. Centurión and J. J. Prías-Barragán, *Nano-Struct. Nano-Objects*, 2020, **24**, 100596.
71. Z. Xu, H. He, S. Zhang, B. Wang, J. Jin, C. Li, X. Chen, B. Jiang and Y. Liu, *Environmental Science: Nano*, 2019, **6**, 1168-1179.
72. Y.-d. Cui, H. Maimaiti, S.-X. Wang, B. Xu, H.-z. Zhang and P.-s. Zhai, *Nano*, 2020, **15**, 2050103.
73. B. Das, A. Girigoswami, P. Pal and S. Dhara, *Mater. Sci. Eng. C*, 2019, **102**, 427-436.
74. S. Chen, M. Chi, Z. Yang, M. Gao, C. Wang and X. Lu, *Inorg. Chem. Front.*, 2017, **4**, 1621-1627.
75. H. Bozetine, Q. Wang, A. Barras, M. Li, T. Hadjersi, S. Szunerits and R. Boukherroub, *J. Colloid Interface Sci.*, 2016, **465**, 286-294.
76. B. De and N. Karak, *J. Mater. Chem. A*, 2017, **5**, 1826-1859.
77. Z. Guo, R. Pan, J. Cheng, L. Zhang, W. Cao and T. He, *Appl. Phys. A*, 2020, **126**, 160.
78. W. Liu, L. Tian, J. Du, J. Wu, Y. Liu, G. Wu and X. Lu, *Analyst*, 2020, **145**, 5500-5507.
79. K. Bhattacharya and P. Deb, *Dalton Trans.*, 2015, **44**, 9221-9229.
80. Q. Xu, W. Cai, M. Zhang, R. Su, Y. Ye, Y. Li, L. Zhang, Y. Guo, Z. Yu, S. Li, X. Lin, Y. Chen, Y. Luo, J. Street and M. Xu, *RSC Adv.*, 2018, **8**, 17254-17262.
81. Q. Xu, Y. Liu, R. Su, L. Cai, B. Li, Y. Zhang, L. Zhang, Y. Wang, Y. Wang and N. Li, *Nanoscale*, 2016, **8**, 17919-17927.
82. Y. Liu, J. Wei, X. Yan, M. Zhao, C. Guo and Q. Xu, *Chin. Chem. Lett.*, 2021, **32**, 861-865.
83. W. Qing, K. Chen, Y. Yang, Y. Wang and X. Liu, *Microchem. J.*, 2020, **152**, 104262.
84. M. Zhang, W. Wang, P. Yuan, C. Chi, J. Zhang and N. Zhou, *Chem. Eng. J.*, 2017, **330**, 1137-1147.
85. H. Yu, Y. Zhao, C. Zhou, L. Shang, Y. Peng, Y. Cao, L.-Z. Wu, C.-H. Tung and T. Zhang, *J. Mater. Chem. A*, 2014, **2**, 3344-3351.

86. Y. Zhu, Z. Wu, M. Jing, H. Hou, Y. Yang, Y. Zhang, X. Yang, W. Song, X. Jia and X. Ji, *J. Mater. Chem. A*, 2015, **3**, 866-877.
87. Z. Zeng, F.-X. Xiao, H. Phan, S. Chen, Z. Yu, R. Wang, T.-Q. Nguyen and T. T. Y. Tan, *J. Mater. Chem. A*, 2018, **6**, 1700-1713.
88. Y. Yang, C. Zhang, D. Huang, G. Zeng, J. Huang, C. Lai, C. Zhou, W. Wang, H. Guo and W. Xue, *Appl. Catal. B-Environ.*, 2019, **245**, 87-99.
89. Y. Wang, L. Mao, W. Liu, F. Ding, P. Zou, X. Wang, Q. Zhao and H. Rao, *Microchim. Acta*, 2018, **185**, 442.
90. B. Wu, Y. Kuang, X. Zhang and J. Chen, *Nano Today*, 2011, **6**, 75-90.
91. Y. Liu, Y. Zhao, Q. Fan, M. S. Khan, X. Li, Y. Zhang, H. Ma and Q. Wei, *Microchim. Acta*, 2018, **185**, 85.
92. Y. Fu, G. Zeng, C. Lai, D. Huang, L. Qin, H. Yi, X. Liu, M. Zhang, B. Li and S. Liu, *Chem. Eng. J.*, 2020, 125743.
93. Q. Huang, H. Zhang, S. Hu, F. Li, W. Weng, J. Chen, Q. Wang, Y. He, W. Zhang and X. Bao, *Biosens. Bioelectron.*, 2014, **52**, 277-280.
94. H. Ge, K. Zhang, H. Yu, J. Yue, L. Yu, X. Chen, T. Hou, K. A. Alamry, H. M. Marwani and S. Wang, *J. Fluoresc.*, 2018, **28**, 1405-1412.
95. H. Zheng, Q. Wang, Y. Long, H. Zhang, X. Huang and R. Zhu, *Chem. Commun.*, 2011, **47**, 10650-10652.
96. X. Wang, Y. Long, Q. Wang, H. Zhang, X. Huang, R. Zhu, P. Teng, L. Liang and H. Zheng, *Carbon*, 2013, **64**, 499-506.
97. S. Mandani, B. Sharma, D. Dey and T. K. Sarma, *Nanoscale*, 2015, **7**, 1802-1808.
98. P. Luo, C. Li and G. Shi, *Phys. Chem. Chem. Phys.*, 2012, **14**, 7360-7366.
99. J. Xu, S. Sahu, L. Cao, C. E. Bunker, G. Peng, Y. Liu, K. A. S. Fernando, P. Wang, E. A. Guliyants, M. J. Meziani, H. Qian and Y.-P. Sun, *Langmuir*, 2012, **28**, 16141-16147.
100. Q. Huang, X. Lin, J.-J. Zhu and Q.-X. Tong, *Biosens. Bioelectron.*, 2017, **94**, 507-512.
101. S. Han, H. Zhang, Y. Xie, L. Liu, C. Shan, X. Li, W. Liu and Y. Tang, *Appl. Surf. Sci.*, 2015, **328**, 368-373.
102. S. A. Rub Pakkath, S. S. Chetty, P. Selvarasu, A. Vadivel Murugan, Y. Kumar, L. Periyasamy, M. Santhakumar, S. R. Sadras and K. Santhakumar, *ACS Biomater. Sci. Eng.*, 2018, **4**, 2582-2596.
103. V. B. Kumar, R. Kumar, A. Gedanken and O. Shefi, *Ultrason. Sonochem.*, 2019, **52**, 205-213.
104. M. Li Liu, B. B. Chen, T. Yang, J. Wang, X. Dong Liu and C. Zhi Huang, *Methods Appl. Fluoresc.*, 2017, **5**, 015003.
105. L. Wu, M. Li, M. Zhang, M. Yan, S. Ge and J. Yu, *Sens. Actuators B Chem.*, 2013, **186**, 761-767.
106. Y. Dong, J. Zhang, P. Jiang, G. Wang, X. Wu, H. Zhao and C. Zhang, *New J. Chem.*, 2015, **39**, 4141-4146.
107. S. Lee, G. Baek, J.-H. Lee, D.-W. Choi, B. Shong and J.-S. Park, *Appl. Surf. Sci.*, 2018, **458**, 864-871.
108. X. Zhang, Z. Sun, Z. Zhu, J. Luo, Z. Wu and Z. Wang, *Ceram. Int.*, 2020.
109. M. Amjadi and R. Jalili, *Biosens. Bioelectron.*, 2017, **96**, 121-126.
110. Q. Li, H. Cheng, X. Wu, C.-F. Wang, G. Wu and S. Chen, *J. Mater. Chem. A*, 2018, **6**, 14112-14119.
111. N. Lim, J.-S. Lee and Y. T. Byun, *Nanomaterials*, 2020, **10**.

112. J. Pan, Y. Sheng, J. Zhang, J. Wei, P. Huang, X. Zhang and B. Feng, *J. Mater. Chem. A*, 2014, **2**, 18082-18086.
113. F. Li, D. Yang and H. Xu, *Chem.-Eur. J.*, 2019, **25**, 1165-1176.
114. Q. Xu, T. Kuang, Y. Liu, L. Cai, X. Peng, T. Sreenivasan Sreeprasad, P. Zhao, Z. Yu and N. Li, *J. Mat. Chem. B*, 2016, **4**, 7204-7219.
115. C. Bie, B. Zhu, F. Xu, L. Zhang and J. Yu, *Adv. Mater.*, 2019, **31**, 1902868.
116. N. A. Travlou, J. Secor and T. J. Bandosz, *Carbon*, 2017, **114**, 544-556.
117. Y. Ma, A. Chen, Y. Huang, X. He, X. Xie, B. He, J. Yang and X. Wang, *Carbon*, 2020, **162**, 234-244.
118. C. V. Raju, G. Kalaiyarasan, S. Paramasivam, J. Joseph and S. S. Kumar, *Electrochim. Acta*, 2020, **331**, 135391.
119. M. Amjadi, T. Hallaj, J. L. Manzoori and T. Shahbazsaghir, *Spectrochim. Acta A Mol. Biomol. Spectrosc.*, 2018, **201**, 223-228.
120. Z. Qian, X. Shan, L. Chai, J. Ma, J. Chen and H. Feng, *ACS Appl. Mater. Interfaces*, 2014, **6**, 6797-6805.
121. P. Long, Y. Feng, C. Cao, Y. Li, J. Han, S. Li, C. Peng, Z. Li and W. Feng, *Adv. Funct. Mater.*, 2018, **28**, 1800791.
122. J. Zhang, D. Nan, S. Pan, H. Liu, H. Yang and X. Hu, *Spectrochim. Acta A Mol. Biomol. Spectrosc.*, 2019, **221**, 117161.
123. A. Pathak, P. Suneesh, J. Stanley and T. S. Babu, *Microchim. Acta*, 2019, **186**, 157.
124. T. Chatzimitakos, A. Kasouni, L. Sygellou, I. Leonardos, A. Troganis and C. Stalikas, *Sens. Actuators B Chem.*, 2018, **267**, 494-501.
125. R. Anjana, J. A. Devi, M. Jayasree, R. Aparna, B. Aswathy, G. Praveen, G. Lekha and G. Sony, *Microchim. Acta*, 2018, **185**, 11.
126. Y. Tu, S. Wang, X. Yuan, Y. Wei, K. Qin, Q. Zhang, X. Chen and X. Ji, *Dyes Pigm.*, 2020, 108316.
127. W. K. Kipnusu, C. Doñate - Buendía, M. Fernández - Alonso, J. Lancis and G. Mínguez - Vega, *Part. Part. Syst. Character.*, 2020, 2000093.
128. T. Tian, Y. He, Y. Ge and G. Song, *Sens. Actuators B Chem.*, 2017, **240**, 1265-1271.
129. S. Huang, E. Yang, J. Yao, Y. Liu and Q. Xiao, *Anal. Chim. Acta*, 2018, **1035**, 192-202.
130. S. Song, J. Hu, M. Li, X. Gong, C. Dong and S. Shuang, *Mater. Sci. Eng. C*, 2021, **118**, 111478.
131. W. Dong, R. Wang, X. Gong, W. Liang, L. Fan, S. Song and C. Dong, *Microchim. Acta*, 2020, **187**, 1-12.
132. Y. Yan, Q. Huang, C. Wei, S. Hu, H. Zhang, W. Zhang, W. Yang, P. Dong, M. Zhu and Z. Wang, *RSC Adv.*, 2016, **6**, 115317-115325.
133. H. Yang, J. Hong, L. Wei and C. Deng, *Ceram. Int.*, 2018, **44**, 16844-16850.
134. H. Li, X. Wang, Z. Cai, L. Lu, J. Tao, B. Sun, Y. Yang, Q. Xu, Z. Yu and P. Zhao, *Anal. Bioanal. Chem.*, 2017, **409**, 6655-6662.
135. X. Li, H. Lin, Q. Li, J. Xue, Y. Xu and L. Zhuang, *ACS Appl. Nano Mater.*, 2021, DOI: 10.1021/acsnm.1c00238.
136. Y. Ye, D. Zhang, Y. Zou, H. Zhao and H. Chen, *J. Clean. Prod.*, 2020, 121682.
137. Y. Wu, Y. Liu, J. Yin, H. Li and J. Huang, *Talanta*, 2019, **205**, 120121.
138. L. L. Pérez, S. Perdriau, G. t. Brink, B. J. Kooi, H. J. Heeres and I. Melián-Cabrera, *Chem. Mater.*, 2013, **25**, 848-855.
139. T. Bala, G. Armstrong, F. Laffir and R. Thornton, *J. Colloid Interface Sci.*, 2011, **356**, 395-403.

140. B. G. Fouda-Mbanga, E. Prabaharan and K. Pillay, *Arab. J. Chem.*, 2020, **13**, 6762-6781.
141. Y. He, J. He, L. Wang, Z. Yu, H. Zhang, Y. Liu and B. Lei, *Sens. Actuators B Chem.*, 2017, **251**, 918-926.
142. Y. He, J. He, H. Zhang, Y. Liu and B. Lei, *J. Colloid Interface Sci.*, 2017, **496**, 8-15.
143. Y. Wang, C. Zhang, X. Chen, B. Yang, L. Yang, C. Jiang and Z. Zhang, *Nanoscale*, 2016, **8**, 5977-5984.
144. W. Wang, E. Eftekhari, G. Zhu, X. Zhang, Z. Yan and Q. Li, *Chem. Commun.*, 2014, **50**, 13089-13092.
145. H. Zhu, W. Zhang, K. Zhang and S. Wang, *Nanotechnology*, 2012, **23**, 315502.
146. Y. Ding, S. Z. Shen, H. Sun, K. Sun and F. Liu, *Sens. Actuators B Chem.*, 2014, **203**, 35-43.
147. Z. Liu, S. Liu, P. Yin and Y. He, *Anal. Chim. Acta*, 2012, **745**, 78-84.
148. B. Cao, C. Yuan, B. Liu, C. Jiang, G. Guan and M.-Y. Han, *Anal. Chim. Acta*, 2013, **786**, 146-152.
149. J. Bai, C. Sun and X. Jiang, *Anal. Bioanal. Chem.*, 2016, **408**, 4705-4714.
150. B. RasulKhan, P. Periakaruppan, S. K. Ponnaiah, G. Venkatachalam and B. Jeyaprabha, *J. Cluster Sci.*, 2021, **32**, 135-144.
151. W. Li, S. Wu, X. Xu, J. Zhuang, H. Zhang, X. Zhang, C. Hu, B. Lei, C. F. Kaminski and Y. Liu, *Chem. Mater.*, 2019, **31**, 9887-9894.
152. W. Suchanek and M. Yoshimura, *J. Mater. Res.*, 1998, **13**, 94-117.
153. Z. Peng, T. Zhao, Y. Zhou, S. Li, J. Li and R. M. Leblanc, *Adv. Healthc. Mater.*, 2020, **9**, 1901495.
154. F. C. Fierz, F. Beckmann, M. Huser, S. H. Irsen, B. Leukers, F. Witte, Ö. Degistirici, A. Andronache, M. Thie and B. Müller, *Biomaterials*, 2008, **29**, 3799-3806.
155. H. K. Chung, V. Wongso, N. S. Sambudi and Isnaeni, *J. Sol-Gel Sci. Technol.*, 2020, **93**, 214-223.
156. M. Irfan, A. Jeshurun, P. Baraneedharan and B. M. Reddy, *Mater. Technol.*, 2021, DOI: 10.1080/10667857.2021.1879529, 1-12.
157. D. Jiang, H. Zhao, Y. Yang, Y. Zhu, X. Chen, J. Sun, K. Yu, H. Fan and X. Zhang, *J. Mat. Chem. B*, 2017, **5**, 3749-3757.
158. S. Gogoi, M. Kumar, B. B. Mandal and N. Karak, *RSC Adv.*, 2016, **6**, 26066-26076.
159. D. K. Khajuria, V. B. Kumar, D. Gigi, A. Gedanken and D. Karasik, *ACS Appl. Mater. Interfaces*, 2018, **10**, 19373-19385.
160. Q. Chang, K. K. Li, S. L. Hu, Y. G. Dong and J. L. Yang, *Mater. Lett.*, 2016, **175**, 44-47.
161. R. Jalili and M. Amjadi, *RSC Adv.*, 2015, **5**, 74084-74090.
162. P.-C. Chen, Y.-N. Chen, P.-C. Hsu, C.-C. Shih and H.-T. Chang, *Chem. Commun.*, 2013, **49**, 1639-1641.
163. A. K. Geim, *Science*, 2009, **324**, 1530-1534.
164. K. Zhou, Y. Zhu, X. Yang, J. Luo, C. Li and S. Luan, *Electrochim. Acta*, 2010, **55**, 3055-3060.
165. X. Geng, L. Niu, Z. Xing, R. Song, G. Liu, M. Sun, G. Cheng, H. Zhong, Z. Liu, Z. Zhang, L. Sun, H. Xu, L. Lu and L. Liu, *Adv. Mater.*, 2010, **22**, 638-642.
166. C.-I. Wang, A. P. Periasamy and H.-T. Chang, *Anal. Chem.*, 2013, **85**, 3263-3270.
167. S. Hu, Q. Huang, Y. Lin, C. Wei, H. Zhang, W. Zhang, Z. Guo, X. Bao, J. Shi and A. Hao, *Electrochim. Acta*, 2014, **130**, 805-809.
168. J. Shin, J. Guo, T. Zhao and Z. Guo, *Small*, 2019, **15**, 1900296.
169. C. Hu, C. Yu, M. Li, X. Wang, Q. Dong, G. Wang and J. Qiu, *Chem. Commun.*, 2015, **51**, 3419-3422.

170. X. Yang, L. Sui, B. Wang, Y. Zhang, Z. Tang, B. Yang and S. Lu, *Sci. China: Chem.*, 2021, **64**, 1547-1553.
171. X. Liu, X. Hu, Z. Xie, P. Chen, X. Sun, J. Yan and S. Zhou, *Anal. Methods*, 2016, **8**, 3236-3241.
172. Q. Chang, X. Meng, S. L. Hu, F. Zhang and J. L. Yang, *RSC Adv.*, 2017, **7**, 30191-30198.
173. M. Massaro, C. G. Colletti, S. Guernelli, G. Lazzara, M. Liu, G. Nicotra, R. Noto, F. Parisi, I. Pibiri, C. Spinella and S. Riela, *J. Mater. Chem. C*, 2018, **6**, 7377-7384.
174. M. Ali, R. Riaz, A. S. Anjum, K. C. Sun, H. Li, S. Ahn, S. H. Jeong and M. J. Ko, *J. Colloid Interface Sci.*, 2021, **586**, 349-361.
175. Z. Shen, C. Zhang, X. Yu, J. Li, Z. Wang, Z. Zhang and B. Liu, *J. Mater. Chem. C*, 2018, **6**, 9636-9641.
176. X. Song, Q. Guo, Z. Cai, J. Qiu and G. Dong, *Ceram. Int.*, 2019, **45**, 17387-17394.
177. C.-C. Shih, P.-C. Chen, G.-L. Lin, C.-W. Wang and H.-T. Chang, *ACS Nano*, 2015, **9**, 312-319.
178. Y.-B. Zhao, Y.-j. Ma, D. Song, Y. Liu, Y. Luo, S. Lin and C.-y. Liu, *Anal. Methods*, 2017, **9**, 4770-4775.
179. A. Konwar, N. Gogoi, G. Majumdar and D. Chowdhury, *Carbohydr. Polym.*, 2015, **115**, 238-245.
180. X. Li, S. Zhang, S. A. Kulinich, Y. Liu and H. Zeng, *Sci. Rep.*, 2014, **4**, 4976.
181. B. Han, W. Wang, H. Wu, F. Fang, N. Wang, X. Zhang and S. Xu, *Colloids Surf. B*, 2012, **100**, 209-214.
182. Z. Yuan, X. Wu, Y. Jiang, Y. Li, J. Huang, L. Hao, J. Zhang and J. Wang, *J. Membr. Sci.*, 2018, **549**, 1-11.
183. Y. Liu, P. Wang, K. S. Fernando, G. E. LeCroy, H. Maimaiti, B. A. Harruff-Miller, W. K. Lewis, C. E. Bunker, Z.-L. Hou and Y.-P. Sun, *J. Mater. Chem. C*, 2016, **4**, 6967-6974.
184. F. Wu, L. Yue, H. Su, K. Wang, L. Yang and X. Zhu, *Nanoscale Res. Lett.*, 2018, **13**, 357.
185. J. Zhang, M. Zheng, F. Zhang, B. Xu, W. Tian and Z. Xie, *Chem. Mater.*, 2016, **28**, 8825-8833.
186. L. Wei, Y. Ma, X. Shi, Y. Wang, X. Su, C. Yu, S. Xiang, L. Xiao and B. Chen, *J. Mat. Chem. B*, 2017, **5**, 3383-3390.
187. X. Zhao, J. Zhang, L. Shi, M. Xian, C. Dong and S. Shuang, *RSC Adv.*, 2017, **7**, 42159-42167.
188. Y. Song, Y. Chen, L. Feng, J. Ren and X. Qu, *Chem. Commun.*, 2011, **47**, 4436-4438.
189. A. Sachdev, I. Matai, S. U. Kumar, B. Bhushan, P. Dubey and P. Gopinath, *RSC Adv.*, 2013, **3**, 16958-16961.
190. N. Arsalani, P. Nezhad-Mokhtari and E. Jabbari, *Artif. Cell. Nanomed. Biotechnol.*, 2019, **47**, 540-547.
191. B.-X. Zhang, G.-Y. Zhang, H. Gao, S.-H. Wu, J.-H. Chen and X.-L. Li, *RSC Adv.*, 2015, **5**, 7395-7400.
192. Z. Peng, C. Ji, Y. Zhou, T. Zhao and R. M. Leblanc, *Appl. Mater. Today*, 2020, **20**, 100677.
193. C.-C. Fu, C.-Y. Wu, C.-C. Chien, T.-H. Hsu, S.-F. Ou, S.-T. Chen, C.-H. Wu, C.-T. Hsieh, R.-S. Juang and Y.-H. Hsueh, *Nanomaterials*, 2020, **10**, 677.
194. A. Sachdev, I. Matai and P. Gopinath, *RSC Adv.*, 2014, **4**, 20915-20921.
195. Y. Dong, R. Wang, H. Li, J. Shao, Y. Chi, X. Lin and G. Chen, *Carbon*, 2012, **50**, 2810-2815.
196. H. Zeng, L. Li, Y. Ding and Q. Zhuang, *Talanta*, 2018, **178**, 879-885.
197. J. J. Huang, Z. F. Zhong, M. Z. Rong, X. Zhou, X. D. Chen and M. Q. Zhang, *Carbon*, 2014, **70**, 190-198.

198. M. C. Kim, K. S. Yu, S. Y. Han, J.-J. Kim, J. W. Lee, N. S. Lee, Y. G. Jeong and D. K. Kim, *Eur. Polym. J.*, 2018, **98**, 191-198.
199. I. Martins, H. Tomás, F. Lahoz and J. Rodrigues, *Biomacromolecules*, 2021, **22**, 2436-2450.
200. Z. Zhu, Z. Sun, Z. Guo, X. Zhang and Z.-c. Wu, *J. Colloid Interface Sci.*, 2019, **552**, 572-582.
201. S. Lu, L. Sui, J. Liu, S. Zhu, A. Chen, M. Jin and B. Yang, *Adv. Mater.*, 2017, **29**, 1603443.
202. B. Wang, J. Li, Z. Tang, B. Yang and S. Lu, *Science Bulletin*, 2019, **64**, 1285-1292.
203. L. Li, D. Liu, H. Mao and T. You, *Biosens. Bioelectron.*, 2017, **89**, 489-495.
204. C. Liu, P. Zhang, X. Zhai, F. Tian, W. Li, J. Yang, Y. Liu, H. Wang, W. Wang and W. Liu, *Biomaterials*, 2012, **33**, 3604-3613.
205. J.-Y. Yin, H.-J. Liu, S. Jiang, Y. Chen and Y. Yao, *ACS Macro Lett.*, 2013, **2**, 1033-1037.
206. H. Liu, Q. Wang, G. Shen, C. Zhang, C. Li, W. Ji, C. Wang and D. Cui, *Nanoscale Res. Lett.*, 2014, **9**, 397.
207. L. Li, T. Zhang, J. Lü and C. Lü, *Appl. Surf. Sci.*, 2018, **454**, 181-191.
208. X. Zhao, W. Shen, Q. Dang, F. Liao, W. Zhu, H. Shi and M. Shao, *J. Appl. Electrochem.*, 2020, **50**, 925-933.
209. D.-Q. Feng, G. Liu, Z. Chen, H. Lu, Y. Gao and X. Fang, *Microchem. J.*, 2020, **157**, 104977.
210. F. Li, C. Liu, J. Yang, Z. Wang, W. Liu and F. Tian, *RSC Adv.*, 2014, **4**, 3201-3205.
211. H. Lv, Y. Yuan, Q. Xu, H. Liu, Y.-G. Wang and Y. Xia, *J. Power Sources*, 2018, **398**, 167-174.
212. Y. Zhou and Z. Ma, *Sens. Actuators B Chem.*, 2016, **233**, 426-430.
213. S. Asadzadeh-Khaneghah, A. Habibi-Yangjeh, D. Seifzadeh, H. Chand and V. Krishnan, *Adv. Powder Technol.*, 2021, **32**, 1196-1206.
214. M. Ganesan, K. D. Ramadhass, H.-C. Chuang and G. Gopalakrishnan, *J. Mol. Liq.*, 2021, **331**, 115768.
215. Y. Liu, C.-y. Liu, Z.-y. Zhang, W.-d. Yang and S.-d. Nie, *J. Mater. Chem. C*, 2015, **3**, 2881-2885.
216. H. Sun, L. Wu, W. Wei and X. Qu, *Mater. Today*, 2013, **16**, 433-442.
217. A. Meng, Q. Xu, K. Zhao, Z. Li, J. Liang and Q. Li, *Sens. Actuators B Chem.*, 2018, **255**, 657-665.
218. Z. Qian, J. Ma, X. Shan, H. Feng, L. Shao and J. Chen, *Chem. Eur. J.*, 2014, **20**, 2254-2263.
219. Y. Liu, P. Wu, X. Wu, C. Ma, S. Luo, M. Xu, W. Li and S. Liu, *Talanta*, 2020, **210**, 120649.
220. T. Liu, N. Li, J. X. Dong, H. Q. Luo and N. B. Li, *Sens. Actuators B Chem.*, 2016, **231**, 147-153.
221. S. Jayaweera, K. Yin, X. Hu and W. J. Ng, *J. Fluoresc.*, 2019, **29**, 1291-1300.
222. L. S. Walekar, P. Hu, F. Liao, X. Guo and M. Long, *Microchim. Acta*, 2018, **185**, 31.
223. W.-S. Zou, W.-L. Kong, Q.-C. Zhao, J. Zhang, X. Zhao, D. Zhao and Y.-Q. Wang, *Microchim. Acta*, 2019, **186**, 576.
224. D. Bano, S. Chandra, P. K. Yadav, V. K. Singh and S. H. Hasan, *J. Photochem. Photobiol. A*, 2020, 112558.
225. S. K. Tammina, Y. Wan, Y. Li and Y. Yang, *J. Photochem. Photobiol. B, Biol.*, 2020, **202**, 111734.
226. M. Li, M. Wang, L. Zhu, Y. Li, Z. Yan, Z. Shen and X. Cao, *Appl. Catal. B-Environ.*, 2018, **231**, 269-276.
227. P. R. Sreenath, S. Mandal, S. Singh, H. Panigrahi, P. Das, A. K. Bhowmick and K. Dinesh Kumar, *Eur. Polym. J.*, 2020, **123**, 109454.
228. J. Deng, Q. Lu, Y. Hou, M. Liu, H. Li, Y. Zhang and S. Yao, *Anal. Chem.*, 2015, **87**, 2195-2203.
229. G. Hong, A. L. Antaris and H. Dai, *Nat. Biomed. Eng.*, 2017, **1**, 0010.
230. R. Weissleder, *Nat. Biotechnol.*, 2001, **19**, 316-317.

231. W. Li, Y. Liu, B. Wang, H. Song, Z. Liu, S. Lu and B. Yang, *Chin. Chem. Lett.*, 2019, **30**, 2323-2327.
232. H. Ali, S. Ghosh and N. R. Jana, *Wiley Interdiscip. Rev.-Nanomed. Nanobiotechnol.*, 2020, **12**, e1617.
233. Z. Xu, J. Liu, K. Wang, B. Yan, S. Hu, X. Ren and Z. Gao, *Environ. Sci. Pollut. Res.*, 2021, DOI: 10.1007/s11356-020-11880-z.
234. Z. Yi, X. Li, H. Zhang, X. Ji, W. Sun, Y. Yu, Y. Liu, J. Huang, Z. Sarshar and M. Sain, *Talanta*, 2021, **222**, 121663.
235. J. Jia, W. Lu, L. Li, Y. Gao, Y. Jiao, H. Han, C. Dong and S. Shuang, *J. Mat. Chem. B*, 2020, **8**, 2123-2127.
236. X. Gong, W. Lu, M. C. Paa, Q. Hu, X. Wu, S. Shuang, C. Dong and M. M. Choi, *Anal. Chim. Acta*, 2015, **861**, 74-84.
237. H. Wang, J. Di, Y. Sun, J. Fu, Z. Wei, H. Matsui, A. del C. Alonso and S. Zhou, *Adv. Funct. Mater.*, 2015, **25**, 5537-5547.
238. S. Huang, E. Yang, Y. Liu, J. Yao, W. Su and Q. Xiao, *Sens. Actuators B Chem.*, 2018, **265**, 326-334.
239. P. Ni, Q. Li, C. Xu, H. Lai, Y. Bai and T. Chen, *Appl. Surf. Sci.*, 2019, **494**, 377-383.
240. L. Yang, W. Jiang, L. Qiu, X. Jiang, D. Zuo, D. Wang and L. Yang, *Nanoscale*, 2015, **7**, 6104-6113.
241. L. Wu, X. Li, Y. Ling, C. Huang and N. Jia, *ACS Appl. Mater. Interfaces*, 2017, **9**, 28222-28232.
242. Y. Rong, C. Wu, J. Yu, X. Zhang, F. Ye, M. Zeigler, M. E. Gallina, I. C. Wu, Y. Zhang, Y.-H. Chan, W. Sun, K. Uvdal and D. T. Chiu, *ACS Nano*, 2013, **7**, 376-384.
243. V. Borse, M. Thakur, S. Sengupta and R. Srivastava, *Sens. Actuators B Chem.*, 2017, **248**, 481-492.
244. R. Atchudan, T. N. J. I. Edison, K. R. Aseer, S. Perumal and Y. R. Lee, *Colloids Surf. B*, 2018, **169**, 321-328.
245. C. Cheng, M. Xing and Q. Wu, *Opt. Mater.*, 2019, **88**, 353-358.
246. D. Qu, X. Miao, X. Wang, C. Nie, Y. Li, L. Luo and Z. Sun, *J. Mat. Chem. B*, 2017, **5**, 4988-4992.
247. L. Zhang, D. Wang, H. Huang, L. Liu, Y. Zhou, X. Xia, K. Deng and X. Liu, *ACS Appl. Mater. Interfaces*, 2016, **8**, 6646-6655.
248. D. J. Bharali, D. W. Lucey, H. Jayakumar, H. E. Pudavar and P. N. Prasad, *J. Am. Chem. Soc.*, 2005, **127**, 11364-11371.
249. N. Parker, M. J. Turk, E. Westrick, J. D. Lewis, P. S. Low and C. P. Leamon, *Anal. Biochem.*, 2005, **338**, 284-293.
250. A. Nasrin, M. Hassan and V. G. Gomes, *Nanoscale*, 2020, **12**, 20598-20603.
251. S. Ruan, J. Qian, S. Shen, J. Zhu, X. Jiang, Q. He and H. Gao, *Nanoscale*, 2014, **6**, 10040-10047.
252. X. Wen, Z. Zhao, S. Zhai, X. Wang and Y. Li, *Diamond Relat. Mater.*, 2020, **105**, 107791.
253. X. Bao, Y. Yuan, J. Chen, B. Zhang, D. Li, D. Zhou, P. Jing, G. Xu, Y. Wang, K. Holá, D. Shen, C. Wu, L. Song, C. Liu, R. Zbořil and S. Qu, *Light: Sci. Appl.*, 2018, **7**, 91.
254. B. B. Karakoçak, J. Liang, S. Kavadiya, M. Y. Berezin, P. Biswas and N. Ravi, *ACS Appl. Nano Mater.*, 2018, **1**, 3682-3692.
255. F. Cui, J. Sun, J. de Dieu Habimana, X. Yang, J. Ji, Y. Zhang, H. Lei, Z. Li, J. Zheng, M. Fan and X. Sun, *Anal. Chem.*, 2019, **91**, 14681-14690.

256. R. Atchudan, T. N. J. I. Edison, S. Perumal, N. Clament Sagaya Selvam and Y. R. Lee, *J. Photochem. Photobiol. A*, 2019, **372**, 99-107.
257. T. Pal, S. Mohiyuddin and G. Packirisamy, *ACS Omega*, 2018, **3**, 831-843.
258. M. Zhang, T. Zheng, B. Sheng, F. Wu, Q. Zhang, W. Wang, J. Shen, N. Zhou and Y. Sun, *Chem. Eng. J.*, 2019, **373**, 1054-1063.
259. L. V. Wang and S. Hu, *Science*, 2012, **335**, 1458-1462.
260. C. Lee, W. Kwon, S. Beack, D. Lee, Y. Park, H. Kim, S. K. Hahn, S.-W. Rhee and C. Kim, *Theranostics*, 2016, **6**, 2196-2208.
261. Q. Jia, J. Ge, W. Liu, S. Liu, G. Niu, L. Guo, H. Zhang and P. Wang, *Nanoscale*, 2016, **8**, 13067-13077.
262. N. Parvin and T. K. Mandal, *Microchim. Acta*, 2017, **184**, 1117-1125.
263. D. Ni, W. Bu, E. B. Ehlerding, W. Cai and J. Shi, *Chem. Soc. Rev.*, 2017, **46**, 7438-7468.
264. R. Di Corato, F. Gazeau, C. Le Visage, D. Fayol, P. Levitz, F. Lux, D. Letourneur, N. Luciani, O. Tillement and C. Wilhelm, *ACS Nano*, 2013, **7**, 7500-7512.
265. Aakash, R. Choubey, D. Das and S. Mukherjee, *J. Alloys Compd.*, 2016, **668**, 33-39.
266. W. A. High, R. A. Ayers, J. Chandler, G. Zito and S. E. Cowper, *J. Am. Acad. Dermatol.*, 2007, **56**, 21-26.
267. H. Wang, X. Na, S. Liu, H. Liu, L. Zhang, M. Xie, Z. Jiang, F. Han, Y. Li, S. Cheng and M. Tan, *Talanta*, 2019, **201**, 388-396.
268. N. Nimi, A. Saraswathy, S. S. Nazeer, N. Francis, S. J. Shenoy and R. S. Jayasree, *Biomaterials*, 2018, **171**, 46-56.
269. S. Sun, L. Zhao, D. Wu, H. Zhang, H. Lian, X. Zhao, A. Wu and L. Zeng, *ACS Appl. Bio Mater.*, 2021, **4**, 1969-1975.
270. F. Du, L. Zhang, L. Zhang, M. Zhang, A. Gong, Y. Tan, J. Miao, Y. Gong, M. Sun, H. Ju, C. Wu and S. Zou, *Biomaterials*, 2017, **121**, 109-120.
271. Y. Wang, T. Wang, X. Chen, Y. Xu and H. Li, *Opt. Mater.*, 2018, **78**, 118-125.
272. A. B. Bourlinos, A. Bakandritsos, A. Kouloumpis, D. Gournis, M. Krysmann, E. P. Giannelis, K. Polakova, K. Safarova, K. Hola and R. Zboril, *J. Mater. Chem.*, 2012, **22**, 23327-23330.
273. H. Liao, Z. Wang, S. Chen, H. Wu, X. Ma and M. Tan, *RSC Adv.*, 2015, **5**, 66575-66581.
274. Y. Wu, H. Li, Y. Yan, K. Wang, Y. Cheng, Y. Li, X. Zhu, J. Xie and X. Sun, *Int. J. Nanomed.*, 2020, **15**, 4691.
275. Y. Zhao, X. Hao, W. Lu, R. Wang, X. Shan, Q. Chen, G. Sun and J. Liu, *ACS Appl. Nano Mater.*, 2018, **1**, 2544-2551.
276. F. Arcamone, G. Franceschi, S. Penco and A. Selva, *Tetrahedron Lett.*, 1969, **10**, 1007-1010.
277. H. Gao, A. V. Sapelkin, M. M. Titirici and G. B. Sukhorukov, *ACS Nano*, 2016, **10**, 9608-9615.
278. T. Feng, X. Ai, H. Ong and Y. Zhao, *ACS Appl. Mater. Interfaces*, 2016, **8**, 18732-18740.
279. P. Gong, J. Du, D. Wang, B. Cao, M. Tian, Y. Wang, L. Sun, S. Ji and Z. Liu, *J. Mat. Chem. B*, 2018, **6**, 2769-2777.
280. T. Yang, J.-L. Huang, Y.-T. Wang, A.-Q. Zheng, Y. Shu and J.-H. Wang, *ChemNanoMat*, 2019, **5**, 479-487.
281. Q. Wang, X. Huang, Y. Long, X. Wang, H. Zhang, R. Zhu, L. Liang, P. Teng and H. Zheng, *Carbon*, 2013, **59**, 192-199.
282. P. Gong, S. Ji, J. Wang, D. Dai, F. Wang, M. Tian, L. Zhang, F. Guo and Z. Liu, *Chem. Eng. J.*, 2018, **348**, 438-446.

283. M. Zhang, P. Yuan, N. Zhou, Y. Su, M. Shao and C. Chi, *RSC Adv.*, 2017, **7**, 9347-9356.
284. P. Gong, L. Sun, F. Wang, X. Liu, Z. Yan, M. Wang, L. Zhang, Z. Tian, Z. Liu and J. You, *Chem. Eng. J.*, 2019, **356**, 994-1002.
285. X. He, Q. Luo, J. Zhang, P. Chen, H.-J. Wang, K. Luo and X.-Q. Yu, *Nanoscale*, 2019, **11**, 12973-12982.
286. X.-Y. Zheng, K. Zhao, J. Tang, X.-Y. Wang, L.-D. Li, N.-X. Chen, Y.-J. Wang, S. Shi, X. Zhang, S. Malaisamy, L.-D. Sun, X. Wang, C. Chen and C.-H. Yan, *ACS Nano*, 2017, **11**, 3642-3650.
287. C.-W. Lai, Y.-H. Hsiao, Y.-K. Peng and P.-T. Chou, *J. Mater. Chem.*, 2012, **22**, 14403-14409.
288. N. Gao, W. Yang, H. Nie, Y. Gong, J. Jing, L. Gao and X. Zhang, *Biosens. Bioelectron.*, 2017, **96**, 300-307.
289. X. Wang, X. Li, Y. Mao, D. Wang, Q. Zhao and S. Wang, *J. Colloid Interface Sci.*, 2019, **552**, 639-650.
290. S. Pandey, M. Thakur, A. Mewada, D. Anjarlekar, N. Mishra and M. Sharon, *J. Mat. Chem. B*, 2013, **1**, 4972-4982.
291. Y.-Y. Yao, G. Gedda, W. M. Girma, C.-L. Yen, Y.-C. Ling and J.-Y. Chang, *ACS Appl. Mater. Interfaces*, 2017, **9**, 13887-13899.
292. X. Jia, Y. Han, M. Pei, X. Zhao, K. Tian, T. Zhou and P. Liu, *Carbohydr. Polym.*, 2016, **152**, 391-397.
293. C. Sarkar, A. R. Chowdhuri, A. Kumar, D. Laha, S. Garai, J. Chakraborty and S. K. Sahu, *Carbohydr. Polym.*, 2018, **181**, 710-718.
294. M. Massaro, G. Barone, G. Biddeci, G. Cavallaro, F. Di Blasi, G. Lazzara, G. Nicotra, C. Spinella, G. Spinelli and S. Riela, *J. Colloid Interface Sci.*, 2019, **552**, 236-246.
295. M. Markman and T. M. Mekhail, *Expert Opin. Pharmacother.*, 2002, **3**, 755-766.
296. X. Wang, W. Zheng, Q. Shen, Y. Wang, Y. Tseng, Z. Luo, X. Wang, L. Shi, C. Li and J. Liu, *Signal Transduct. Target. Ther.*, 2021, **6**, 33.
297. I. J. Gomez, B. Arnaiz, M. Cacioppo, F. Arcudi and M. Prato, *J. Mat. Chem. B*, 2018, **6**, 5540-5548.
298. K. C. Nicolaou, W.-M. Dai and R. K. Guy, *Angew. Chem.-Int. Edit.*, 1994, **33**, 15-44.
299. P. Ye, J. Chang, L. F. Foo and B. C. M. Yap, *Int. J. Oral Sci.*, 2017, **9**, 167-173.
300. S. M. Ardekani, A. Dehghani, P. Ye, K.-A. Nguyen and V. G. Gomes, *J. Colloid Interface Sci.*, 2019, **552**, 378-387.
301. X. He, P. Chen, J. Zhang, T.-Y. Luo, H.-J. Wang, Y.-H. Liu and X.-Q. Yu, *Biomater. Sci.*, 2019, **7**, 1940-1948.
302. K. Zhang, G. Ma, H. Wang, Z. Liang, L. Zhou and B. Yan, *J. Mater. Sci.*, 2021, **56**, 4396-4406.
303. S. Singh, A. Mishra, R. Kumari, K. K. Sinha, M. K. Singh and P. Das, *Carbon*, 2017, **114**, 169-176.
304. K. Kamimura, T. Suda, G. Zhang and D. Liu, *Pharm Biol*, 2011, **25**, 293-306.
305. S. O. Han, R. I. Mahato, Y. K. Sung and S. W. Kim, *Mol. Ther.*, 2000, **2**, 302-317.
306. B. Wang, J. Huang, M. Zhang, Y. Wang, H. Wang, Y. Ma, X. Zhao, X. Wang, C. Liu, H. Huang, Y. Liu, F. Lu, H. Yu, M. Shao and Z. Kang, *ACS Appl. Bio Mater.*, 2020, **3**, 8857-8864.
307. P. Chen, J. Zhang, X. He, Y.-H. Liu and X.-Q. Yu, *Biomater. Sci.*, 2020, **8**, 3730-3740.
308. Q. Wang, C. Zhang, G. Shen, H. Liu, H. Fu and D. Cui, *J. Nanobiotechnol*, 2014, **12**, 58.
309. W. T. Godbey, K. K. Wu and A. G. Mikos, *J. Control. Release*, 1999, **60**, 149-160.
310. L. Shen, L. Zhang, M. Chen, X. Chen and J. Wang, *Carbon*, 2013, **55**, 343-349.

311. L. Hu, Y. Sun, S. Li, X. Wang, K. Hu, L. Wang, X.-j. Liang and Y. Wu, *Carbon*, 2014, **67**, 508-513.
312. Q. Dou, X. Fang, S. Jiang, P. L. Chee, T.-C. Lee and X. J. Loh, *RSC Adv.*, 2015, **5**, 46817-46822.
313. Y. Hu, X. Geng, L. Zhang, Z. Huang, J. Ge and Z. Li, *Sci. Rep.*, 2017, **7**, 5849.
314. C. Mickaël, F. Jiahui, R. Mickaël, P. Françoise and L. Luc, *RSC Adv.*, 2019, **9**, 3493-3502.
315. K. Yang, M. Liu, Y. Wang, S. Wang, H. Miao, L. Yang and X. Yang, *Sens. Actuators B Chem.*, 2017, **251**, 503-508.
316. T.-Y. Luo, X. He, J. Zhang, P. Chen, Y.-H. Liu, H.-J. Wang and X.-Q. Yu, *RSC Adv.*, 2018, **8**, 6053-6062.
317. W. Liu, L. Tian, J. Du, J. Wu, Y. Liu, G. Wu and X. Lu, *The Analyst*, 2020.
318. T. Vo-Dinh and B. Cullum, *Fresenius J. Anal. Chem.*, 2000, **366**, 540-551.
319. F.-T. Wang, L.-N. Wang, J. Xu, K.-J. Huang and X. Wu, *Analyst*, 2021, **146**, 4418-4435.
320. X. Sun and Y. Lei, *TrAC, Trends Anal. Chem.*, 2017, **89**, 163-180.
321. Z. Yang, Z. Li, M. Xu, Y. Ma, J. Zhang, Y. Su, F. Gao, H. Wei and L. Zhang, *Nano-Micro Lett.*, 2013, **5**, 247-259.
322. H. Shi, J. Wei, L. Qiang, X. Chen and X. Meng, *J. Biomed. Nanotechnol.*, 2014, **10**, 2677-2699.
323. W. Ye, Y. Zhang, W. Hu, L. Wang, Y. Zhang and P. Wang, *Nanomaterials*, 2020, **10**.
324. L. Wang, H.-X. Cao, Y.-S. He, C.-G. Pan, T.-K. Sun, X.-Y. Zhang, C.-Y. Wang and G.-X. Liang, *Sens. Actuators B Chem.*, 2019, **282**, 78-84.
325. X. Fu, L. Sheng, Y. Yu, M. Ma, Z. Cai and X. Huang, *Sens. Actuators B Chem.*, 2018, **269**, 278-287.
326. X. Wang, D. Wang, Y. Guo, C. Yang, A. Iqbal, W. Liu, W. Qin, D. Yan and H. Guo, *Dalton Trans.*, 2015, **44**, 5547-5554.
327. X. Wu, S. Sun, Y. Wang, J. Zhu, K. Jiang, Y. Leng, Q. Shu and H. Lin, *Biosens. Bioelectron.*, 2017, **90**, 501-507.
328. I. Costas-Mora, V. Romero, I. Lavilla and C. Bendicho, *Anal. Chem.*, 2014, **86**, 4536-4543.
329. S. Ganguly, P. Das, S. Das, U. Ghorai, M. Bose, S. Ghosh, M. Mondal, A. K. Das, S. Banerjee and N. C. Das, *Colloids Surf. Physicochem. Eng. Aspects*, 2019, **579**, 123604.
330. A. Barati, M. Shamsipur and H. Abdollahi, *Biosens. Bioelectron.*, 2015, **71**, 470-475.
331. J. Wang, Y. Wu, P. Zhou, W. Yang, H. Tao, S. Qiu and C. Feng, *Analyst*, 2018, **143**, 5151-5160.
332. C. Han, R. Wang, K. Wang, H. Xu, M. Sui, J. Li and K. Xu, *Biosens. Bioelectron.*, 2016, **83**, 229-236.
333. S. K. Tammina and Y. Yang, *J. Photochem. Photobiol. A*, 2020, **387**, 112134.
334. X. Yan, Y. Song, C. Zhu, H. Li, D. Du, X. Su and Y. Lin, *Anal. Chem.*, 2018, **90**, 2618-2624.
335. F. Khakbaz and M. Mahani, *Anal. Biochem.*, 2017, **523**, 32-38.
336. J. Zhang, X. Zhao, M. Xian, C. Dong and S. Shuang, *Talanta*, 2018, **183**, 39-47.
337. Z. Zhu, X. Lin, L. Wu, C. Zhao, Y. Zheng, A. Liu, L. Lin and X. Lin, *Sens. Actuators B Chem.*, 2018, **274**, 609-615.
338. Y.-T. Yen, Y.-S. Lin, T.-Y. Chen, S.-C. Chyueh and H.-T. Chang, *Royal Soc. Open Sci.*, **6**, 191017.
339. S. Liu, J. Cui, J. Huang, B. Tian, F. Jia and Z. Wang, *Spectrochim. Acta A Mol. Biomol. Spectrosc.*, 2019, **206**, 65-71.
340. H. Cai, Y. Zhu, H. Xu, H. Chu, D. Zhang and J. Li, *Spectrochim. Acta A Mol. Biomol. Spectrosc.*, 2021, **246**, 119033.
341. H. Wang, S. Liu, Y. Xie, J. Bi, Y. Li, Y. Song, S. Cheng, D. Li and M. Tan, *New J. Chem.*, 2018, **42**, 3729-3735.

342. H. Sies, *Redox Biol.*, 2015, **4**, 180-183.
343. L. Li, L. Shi, J. Jia, O. Eltayeb, W. Lu, Y. Tang, C. Dong and S. Shuang, *ACS Appl. Mater. Interfaces*, 2020, **12**, 18250-18257.
344. D. Wu, G. Li, X. Chen, N. Qiu, X. Shi, G. Chen, Z. Sun, J. You and Y. Wu, *Microchim. Acta*, 2017, **184**, 1923-1931.
345. M. He, N. Shang, B. Zheng and G. Yue, *RSC Adv.*, 2021, **11**, 21137-21144.
346. Q.-Y. Cai, J. Li, J. Ge, L. Zhang, Y.-L. Hu, Z.-H. Li and L.-B. Qu, *Biosens. Bioelectron.*, 2015, **72**, 31-36.
347. C. Yang, W. Deng, H. Liu, S. Ge and M. Yan, *Sens. Actuators B Chem.*, 2015, **216**, 286-292.
348. F. Abedini, H. Hosseinkhani, M. Ismail, A. J. Domb, A. R. Omar, P. P. Chong, P.-D. Hong, D.-S. Yu and I.-Y. Farber, *Int. J. Nanomed.*, 2012, **7**, 4159-4168.
349. Y. Zhang, Y. Nie, R. Zhu, D. Han, H. Zhao and Z. Li, *Talanta*, 2019, **204**, 74-81.
350. A. H. Loo, Z. Sofer, D. Bouša, P. Ulbrich, A. Bonanni and M. Pumera, *ACS Appl. Mater. Interfaces*, 2016, **8**, 1951-1957.
351. Y. Wang, S. Wang, S. Ge, S. Wang, M. Yan, D. Zang and J. Yu, *Anal. Methods*, 2013, **5**, 1328-1336.
352. S. H. Qaddare and A. Salimi, *Biosens. Bioelectron.*, 2017, **89**, 773-780.
353. J. Kudr, L. Richtera, K. Xhaxhiu, D. Hynek, Z. Heger, O. Zitka and V. Adam, *Biosens. Bioelectron.*, 2017, **92**, 133-139.
354. S.-S. Liang, L. Qi, R.-L. Zhang, M. Jin and Z.-Q. Zhang, *Sens. Actuators B Chem.*, 2017, **244**, 585-590.
355. N. Li, S. G. Liu, Y. D. Zhu, T. Liu, S. M. Lin, Y. Shi, H. Q. Luo and N. B. Li, *Sens. Actuators B Chem.*, 2017, **251**, 455-461.
356. Q. Huang, Q. Li, Y. Chen, L. Tong, X. Lin, J. Zhu and Q. Tong, *Sens. Actuators B Chem.*, 2018, **276**, 82-88.
357. Z. Wu, R. Chen, S. Pan, H. Liu and X. Hu, *Microchem. J.*, 2021, **164**, 105976.
358. X. Cheng, Y. Cen, G. Xu, F. Wei, M. Shi, X. Xu, M. Sohail and Q. Hu, *Microchim. Acta*, 2018, **185**, 144.
359. S. Xu, F. Zhang, L. Xu, X. Liu, P. Ma, Y. Sun, X. Wang and D. Song, *Sens. Actuators B Chem.*, 2018, **273**, 1015-1021.
360. H. Zhu, E. Wang, J. Li and J. Wang, *Anal. Chim. Acta*, 2018, **1006**, 83-89.
361. M. Amjadi, T. Hallaj and Z. Kouhi, *J. Photochem. Photobiol. A*, 2018, **356**, 603-609.
362. Q. Huang, X. Lin, C. Lin, Y. Zhang, S. Hu and C. Wei, *RSC Adv.*, 2015, **5**, 54102-54108.
363. Q. Huang, S. Hu, H. Zhang, J. Chen, Y. He, F. Li, W. Weng, J. Ni, X. Bao and Y. Lin, *Analyst*, 2013, **138**, 5417-5423.
364. Q. Ye, F. Yan, D. Shi, T. Zheng, Y. Wang, X. Zhou and L. Chen, *J. Photochem. Photobiol. B, Biol.*, 2016, **162**, 1-13.
365. C. Li, Y. Wang, X. Zhang, X. Guo, X. Kang, L. Du and Y. Liu, *J. Colloid Interface Sci.*, 2018, **526**, 487-496.
366. F. Yang, J. R. Wild and A. J. Russell, *Biotechnol. Progr.*, 1995, **11**, 471-474.
367. X. Gao, G. Tang and X. Su, *Biosens. Bioelectron.*, 2012, **36**, 75-80.
368. J. Hou, J. Dong, H. Zhu, X. Teng, S. Ai and M. Mang, *Biosens. Bioelectron.*, 2015, **68**, 20-26.
369. R. P. Deo, J. Wang, I. Block, A. Mulchandani, K. A. Joshi, M. Trojanowicz, F. Scholz, W. Chen and Y. Lin, *Anal. Chim. Acta*, 2005, **530**, 185-189.

370. J. Hou, Z. Tian, H. Xie, Q. Tian and S. Ai, *Sens. Actuators B Chem.*, 2016, **232**, 477-483.
371. B. Chen, S. Chai, J. Liu, C. Liu, Y. Li, J. He, Z. Yu, T. Yang, C. Feng and C. Huang, *Anal. Bioanal. Chem.*, 2019, **411**, 2291-2300.
372. X. Wang, Y. Liu, Q. Zhou, X. Sheng, Y. Sun, B. Zhou, J. Zhao and J. Guo, *Sci. Total Environ.*, 2020, **720**, 137680.
373. D. Shi, F. Yan, T. Zheng, Y. Wang, X. Zhou and L. Chen, *RSC Adv.*, 2015, **5**, 98492-98499.
374. X. Wang, X. Li, X. Li, Y. Wang, Q. Han and J. Li, *Anal. Chim. Acta*, 2020, **1098**, 170-180.
375. K. Gao, Y. Guo, Q. Niu, L. Han, L. Zhou and L. Wang, *Sens. Actuators B Chem.*, 2018, **262**, 298-305.
376. G. Yue, S. Li, W. Liu, F. Ding, P. Zou, X. Wang, Q. Zhao and H. Rao, *Sens. Actuators B Chem.*, 2019, **287**, 408-415.
377. N. Xiao, S. G. Liu, S. Mo, Y. Z. Yang, L. Han, Y. J. Ju, N. B. Li and H. Q. Luo, *Sens. Actuators B Chem.*, 2018, **273**, 1735-1743.
378. C. Wang, Z. Xu and C. Zhang, *ChemNanoMat*, 2015, **1**, 122-127.
379. M. Omid, A. Yadegari and L. Tayebi, *RSC Adv.*, 2017, **7**, 10638-10649.
380. Y. Ma, Y. Cen, M. Sohail, G. Xu, F. Wei, M. Shi, X. Xu, Y. Song, Y. Ma and Q. Hu, *ACS Appl. Mater. Interfaces*, 2017, **9**, 33011-33019.
381. Y. Gong, B. Yu, W. Yang and X. Zhang, *Biosens. Bioelectron.*, 2016, **79**, 822-828.
382. W. Shi, F. Guo, M. Han, S. Yuan, W. Guan, H. Li, H. Huang, Y. Liu and Z. Kang, *J. Mat. Chem. B*, 2017, **5**, 3293-3299.
383. J. Zhang, H. Yang, S. Pan, H. Liu and X. Hu, *Spectrochim. Acta A Mol. Biomol. Spectrosc.*, 2021, **244**, 118831.
384. N. Jing, M. Tian, Y. Wang and Y. Zhang, *J. Lumin.*, 2019, **206**, 169-175.
385. D. Y. Li, S. P. Wang, F. Azad and S. C. Su, *Ecotoxicol. Environ. Saf.*, 2020, **190**, 110141.
386. K. M. Omer and A. Q. Hassan, *Microchim. Acta*, 2017, **184**, 2063-2071.
387. L. Li, B. Yu and T. You, *Biosens. Bioelectron.*, 2015, **74**, 263-269.
388. F. Yan, Z. Bai, Y. Chen, F. Zu, X. Li, J. Xu and L. Chen, *Sens. Actuators B Chem.*, 2018, **275**, 86-94.
389. J. Chen, Y. Li, K. Lv, W. Zhong, H. Wang, Z. Wu, P. Yi and J. Jiang, *Sens. Actuators B Chem.*, 2016, **224**, 298-306.
390. H. N. Abdelhamid, A. Talib and H.-F. Wu, *Talanta*, 2017, **166**, 357-363.
391. H.-Y. Zhang, Y. Wang, S. Xiao, H. Wang, J.-H. Wang and L. Feng, *Biosens. Bioelectron.*, 2017, **87**, 46-52.
392. J. An, R. Chen, M. Chen, Y. Hu, Y. Lyu and Y. Liu, *Sens. Actuators B Chem.*, 2021, **329**, 129097.
393. H. Guo, X. Wang, N. Wu, M. Xu, M. Wang, L. Zhang and W. Yang, *Anal. Methods*, 2020, **12**, 4058-4063.
394. Y. Kim and J. Kim, *Opt. Mater.*, 2020, **99**, 109514.
395. W. J. Zhang, S. G. Liu, L. Han, H. Q. Luo and N. B. Li, *Sens. Actuators B Chem.*, 2019, **283**, 215-221.
396. M. Zhang, R. Su, J. Zhong, L. Fei, W. Cai, Q. Guan, W. Li, N. Li, Y. Chen and L. Cai, *Nano Res.*, 2019, **12**, 815-821.
397. Y. Zhang, X. Fang, H. Zhao and Z. Li, *Talanta*, 2018, **181**, 318-325.
398. A. Kumar, A. R. Chowdhuri, D. Laha, T. K. Mahto, P. Karmakar and S. K. Sahu, *Sens. Actuators B Chem.*, 2017, **242**, 679-686.

399. Y. Jiang, Y. Wang, F. Meng, B. Wang, Y. Cheng and C. Zhu, *New J. Chem.*, 2015, **39**, 3357-3360.
400. Q. Ye, F. Yan, Y. Luo, Y. Wang, X. Zhou and L. Chen, *Spectrochim. Acta A Mol. Biomol. Spectrosc.*, 2017, **173**, 854-862.
401. F. Wang, Q. Hao, Y. Zhang, Y. Xu and W. Lei, *Microchim. Acta*, 2016, **183**, 273-279.
402. L. Li, Y. Li, Y. Ye, R. Guo, A. Wang, G. Zou, H. Hou and X. Ji, *ACS Nano*, 2021, **15**, 6872-6885.
403. X. Niu, T. Song and H. Xiong, *Chin. Chem. Lett.*, 2021, **32**, 1953-1956.
404. I. Garner, R. Vichare, R. Paulson, R. Appavu, S. K. Panguluri, R. Tzekov, N. Sahiner, R. Ayyala and M. R. Biswal, *Front. Bioeng. Biotechnol.*, 2020, **8**, 1139.
405. Y. Park, Y. Kim, H. Chang, S. Won, H. Kim and W. Kwon, *J. Mat. Chem. B*, 2020, **8**, 8935-8951.
406. K. Wang, Z. Gao, G. Gao, Y. Wo, Y. Wang, G. Shen and D. Cui, *Nanoscale Res. Lett.*, 2013, **8**, 122.
407. Q. Xu, J. Gao, S. Wang, Y. Wang, D. Liu and J. Wang, *J. Mat. Chem. B*, 2021, **9**, 5765-5779.
408. N. Vale, S. Silva, D. Duarte, D. M. A. Crista, L. Pinto da Silva and J. C. G. Esteves da Silva, *RSC Med. Chem.*, 2021, **12**, 245-253.